LETTER

https://doi.org/10.1038/s41586-018-0104-4

Cellular milieu imparts distinct pathological α-synuclein strains in α-synucleinopathies

Chao Peng, Ronald J. Gathagan, Dustin J. Covell, Coraima Medellin, Anna Stieber, John L. Robinson, Bin Zhang, Rose M. Pitkin, Modupe F. Olufemi, Kelvin C. Luk, John Q. Trojanowski & Virginia M.-Y. Lee*

In Lewy body diseases—including Parkinson's disease, without or with dementia, dementia with Lewy bodies, and Alzheimer's disease with Lewy body co-pathology[1]—α-synuclein (α-Syn) aggregates in neurons as Lewy bodies and Lewy neurites[2]. By contrast, in multiple system atrophy α-Syn accumulates mainly in oligodendrocytes as glial cytoplasmic inclusions (GCIs)[3]. Here we report that pathological α-Syn in GCIs and Lewy bodies (GCI-α-Syn and LB-α-Syn, respectively) is conformationally and biologically distinct. GCI-α-Syn forms structures that are more compact and it is about 1,000-fold more potent than LB-α-Syn in seeding α-Syn aggregation, consistent with the highly aggressive nature of multiple system atrophy. GCI-α-Syn and LB-α-Syn show no cell-type preference in seeding α-Syn pathology, which raises the question of why they demonstrate different cell-type distributions in Lewy body disease versus multiple system atrophy. We found that oligodendrocytes but not neurons transform misfolded α-Syn into a GCI-like strain, highlighting the fact that distinct α-Syn strains are generated by different intracellular milieus. Moreover, GCI-α-Syn maintains its high seeding activity when propagated in neurons. Thus, α-Syn strains are determined by both misfolded seeds and intracellular environments.

The diverse nature of α-synucleinopathies suggests that they may be caused by distinct α-Syn strains[4–8]. To investigate whether GCI-α-Syn and LB-α-Syn represent two distinct strains, sarkosyl-insoluble α-Syn was isolated from the brains of patients with multiple system atrophy (MSA), which exists as two subtypes—the Parkinsonian subtype (MSA-P) and the cerebellar subtype (MSA-C)[9, 10]—and brains from patients with Lewy body disease (Extended Data Fig. 1a and Supplementary Tables 1, 2). First we evaluated the extent of Ser129 phosphorylation (pS129), which is a hallmark of pathological α-Syn[11, 12], on GCI-α-Syn and LB-α-Syn, and found much less pS129 on GCI-α-Syn than on LB-α-Syn (Fig. 1a, b). Second, we analysed conformational differences between GCI-α-Syn and LB-α-Syn using proteinase K digestion. Proteinase K digestion shows predominantly undigested α-Syn for GCI-α-Syn (1st band in Fig. 1c), whereas LB-α-Syn was cleaved into smaller fragments (2nd–4th bands in Fig. 1c). The relative resistance of GCI-α-Syn to proteinase K digestion was further confirmed using increasing concentrations of proteinase K (Fig. 1d), which indicates that GCI-α-Syn might form a more-compact structure than LB-α-Syn. Epitope mapping showed that the 2nd band after proteinase K digestion was truncated mainly at the N terminus, whereas the 3rd and 4th bands were truncated mainly at the C terminus (Extended Data Fig. 1b, c). GCI-α-Syn and LB-α-Syn also produced distinct banding patterns when digested with trypsin or thermolysin, further demonstrating their different conformations (Extended Data Fig. 1d–g).

To confirm that GCI-α-Syn and LB-α-Syn have different conformations, we immunostained sections of diseased brains with the monoclonal antibody (MAb) Syn7015, which is selective for a synthetic α-Syn strain[13]. At low concentrations Syn7015 preferentially recognized GCIs over Lewy bodies, whereas another MAb Syn303 that detects pathological α-Syn[13, 14] immunostained GCIs and Lewy bodies equally well (Extended Data Fig. 2a, b). Semi-quantitative analyses of Lewy bodies and GCIs[15, 16] stained by Syn7015 or Syn303 on adjacent sections showed that Syn7015 preferentially recognized GCIs over Lewy bodies (Fig. 1e), which was also supported by the ratio of total area occupied by Syn7015-positive over Syn303-positive pathology (Fig. 1f, g and Extended Data Fig. 2c). This preferential recognition further demonstrates that there are conformational differences between GCI-α-Syn and LB-α-Syn.

To determine whether structural differences between GCI-α-Syn and LB-α-Syn influence their seeding activities, we treated primary oligodendrocytes expressing α-Syn with an equal amount of GCI-α-Syn, LB-α-Syn or α-Syn preformed fibrils (PFFs)[17]. GCI-α-Syn is much more potent than LB-α-Syn and PFFs at seeding α-Syn aggregation in oligodendrocytes (Fig. 1h, i and Extended Data Fig. 3a, b). Specifically, GCI-α-Syn is approximately 1,000-fold more potent than LB-α-Syn and PFFs (Fig. 1j): 30 ng of LB-α-Syn induced a similar amount of pathology as 30 pg of GCI-α-Syn, and 30 μg of PFFs were comparable to 30 ng of GCI-α-Syn. The purity of the oligodendrocyte cultures and the presence of α-Syn pathology in oligodendrocytes were confirmed by immunofluorescence staining (Extended Data Fig. 3c–f).

Because the high potency of GCI-α-Syn in inducing oligodendrocyte pathology is consistent with the distribution of this strain in oligodendrocytes of patients with MSA, we hypothesized that the properties of GCI-α-Syn and LB-α-Syn dictate their differential cell-type distribution in patients (hypothesis 1 in Extended Data Fig. 3g), and speculated that LB-α-Syn is more potent than GCI-α-Syn in inducing neuronal pathology. Primary neurons treated with GCI-α-Syn developed many more α-Syn inclusions than those treated with LB-α-Syn or PFFs (Fig. 2a, b and Extended Data Fig. 4a, b), and GCI-α-Syn also was about 1,000-fold more potent than LB-α-Syn or PFFs in inducing neuronal α-Syn pathology (Fig. 2c, d). Furthermore, using a QBI-293 cell line expressing human α-Syn (hereafter, 'QBI-WT-Syn' cells)[18], we confirmed that GCI-α-Syn is about 1,000-fold more potent than LB-α-Syn and PFFs (Fig. 2e, f and Extended Data Fig. 4c–e). To rule out possible contributions of contaminating proteins, GCI-α-Syn and LB-α-Syn were further purified by immunoprecipitation. Immunoprecipitation-purified GCI-α-Syn maintained its markedly higher seeding ability compared to LB-α-Syn (Extended Data Fig. 4f). Moreover, the addition of PFFs to immunoprecipitation-depleted GCI-α-Syn preparations did not increase the seeding ability of PFFs (Extended Data Fig. 4g, h).

Because GCI-α-Syn is more resistant to proteinase K digestion (Fig. 1c, d), we investigated whether the high potency of GCI-α-Syn is due to its resistance to degradation. Previously we showed that exogenously added misfolded α-Syn accumulates in lysosomes and that treating the cells with chloroquine (a lysosomal inhibitor) could increase the amount of α-Syn pathology that was induced[19]. To test this hypothesis, primary neurons seeded with GCI-α-Syn, LB-α-Syn or PFFs were treated with chloroquine. Chloroquine treatment similarly increased the pathology induced by GCI-α-Syn, LB-α-Syn and PFFs (Extended

The Department of Pathology and Laboratory Medicine, Institute on Aging and Center for Neurodegenerative Disease Research, the Perelman School of Medicine at the University of Pennsylvania, Philadelphia, PA, USA. *e-mail: vmylee@upenn.edu

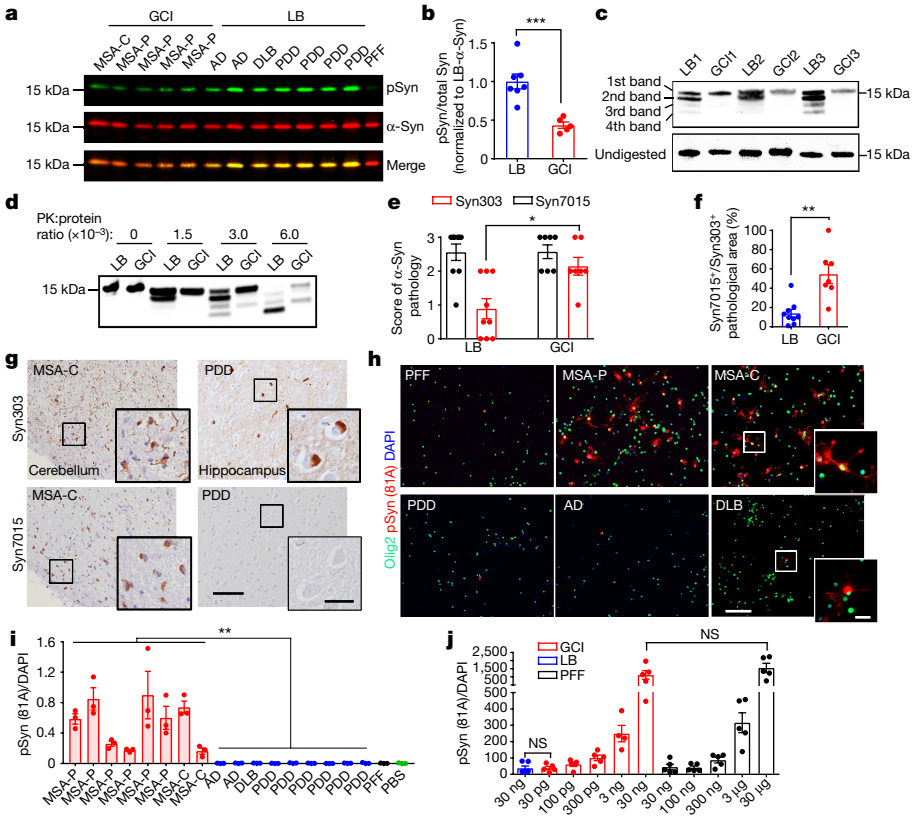

Fig. 1 | GCI-α-Syn and LB-α-Syn represent two distinct strains. **a**, GCI and Lewy body immunoblotted with antibodies against total α-Syn or pS129 α-Syn (pSyn). **b**, Quantification of pS129 α-Syn versus total α-Syn shown in **a** (GCI, $n = 5$ cases; LB, $n = 7$ cases). **c**, Proteinase K-digested LB-α-Syn and GCI-α-Syn from six cases immunoblotted with anti-α-Syn MAb (Syn211). **d**, GCI-α-Syn and LB-α-Syn incubated with increasing concentrations of proteinase K (PK) and immunoblotted with Syn211 (experiment repeated three times). **e**, Semi-quantitative scores (0–3) to quantify α-Syn pathology revealed by Syn303 or Syn7015 immunohistochemistry in adjacent brain sections of patients with MSA or Lewy body disease (LB, $n = 9$ cases; GCI, $n = 7$ cases) (statistics: Mann–Whitney *U*-test). **f**, Quantification of area occupied by Syn7015-positive (Syn7015$^+$) versus Syn303-positive (Syn303$^+$) α-Syn pathology for experiments in **e** (LB, $n = 9$ cases, GCI, $n = 7$ cases). **g**, Representative photomicrographs for experiments in **e** (repeated with seven cases). **h**, Primary oligodendrocytes expressing α-Syn-mCherry incubated with 13 ng GCI-α-Syn, LB-α-Syn or PFFs were stained with 81A (pS129 α-Syn) and anti-olig2 (experiment repeated four times). **i**, Quantification of pS129 α-Syn induced by GCI-α-Syn, LB-α-Syn and PFF in oligodendrocytes expressing α-Syn (GCI, $n = 8$ different preparations; LB, $n = 9$ different preparations) (statistics: two-tailed unpaired *t*-test using the mean value of each case). **j**, Quantification of pS129 α-Syn induced by various amounts of PFFs, GCI-α-Syn or LB-α-Syn in oligodendrocytes expressing α-Syn ($n = 6$ (LB), 4 (GCI 3 ng) or 5 (all other groups) biological replicates) (statistics: adjusted with Bonferroni correction). Results shown as mean ± s.e.m. $^*P < 0.05$; $^{**}P < 0.01$; $^{***}P < 0.001$; $^{****}P < 0.0001$; NS, not significant. Scale bars: 100 μm (**g**, **h**), 25 μm (**g** inset), 10 μm (**h** inset). AD, Alzheimer's disease; DLB, dementia with Lewy bodies; LB, Lewy body; PDD, Parkinson's disease with dementia. For gel source data, see Supplementary Fig. 1. See Supplementary Table 5 for statistical details.

Data Fig. 4i, j), which suggests that the high potency of GCI-α-Syn is not likely to be due to its resistance to lysosomal proteolysis.

The markedly different seeding abilities of GCI-α-Syn and LB-α-Syn in vitro prompted us to test their properties in vivo. Equivalent amounts of GCI-α-Syn or LB-α-Syn were injected into the striatum of wild-type mice[20]. At three months post-injection, only GCI-α-Syn-injected wild-type (GCI-WT) mice developed abundant neuronal inclusions (Fig. 2g). At six months post-injection, although the amount of α-Syn pathology in GCI-WT mice declined markedly, only a limited number of neurons developed α-Syn pathology in LB-α-Syn-injected wild-type (LB-WT) mice (Extended Data Fig. 4k). Therefore, GCI-α-Syn more-potently induces neuronal pathology in vivo, which also argues against cell-type specific seeding by GCI-α-Syn. Furthermore, no oligodendroglial pathology was detected in GCI-WT mice, which further argues against the hypothesis that the properties of GCI-α-Syn dictate its oligodendrocyte distribution. On the other hand, the high potency of GCI-α-Syn probably contributes to the aggressive nature of MSA.

Misfolded α-Syn was shown to spread through the neuroanatomical connectome, but how the properties of different α-Syn strains affect this spreading process is unclear. We compared the transmission pattern of α-Syn pathology in wild-type mice injected with GCI-α-Syn, LB-α-Syn or PFFs. GCI-α-Syn spread more efficiently to the entorhinal cortex, hippocampus and pyramidal layer of piriform cortex, but less efficiently to other cortical regions such as the motor cortex, as compared to PFFs and LB-α-Syn (Fig. 2h, i and Extended Data Figs. 4l, 5a, b). By contrast, PFFs induced relatively more pathology in the striatum and substantia nigra but less in the olfactory bulb, as compared with LB-α-Syn and GCI-α-Syn (Fig. 2h, i and Extended Data Figs. 4l, 5a, b). Therefore, our data demonstrate that different α-Syn strains markedly modulate their transmission patterns in the nervous system.

The observation that the seeding properties of GCI-α-Syn and LB-α-Syn do not show any cell-type preference raises the question of why they demonstrate distinct cell-type distributions in diseased brains. Because our data argue against the hypothesis that strain properties determine cell-type distributions (hypothesis 1 in Extended Data Fig. 3g), we proposed an alternative hypothesis that the different cellular environments of neurons and oligodendrocytes promote the formation of distinct α-Syn strains (hypothesis 2 in Extended Data Fig. 3g). According to this hypothesis, injection of LB-α-Syn into mice expressing α-Syn in oligodendrocytes should convert the LB-α-Syn into a GCI-like strain. To test this hypothesis and to eliminate confounding factors arising from neuronal pathology, we crossed 2′,3′-cyclic nucleotide 3′ phosphodiesterase (CNP)-α-Syn transgenic mice (M2 line)[21] with α-Syn

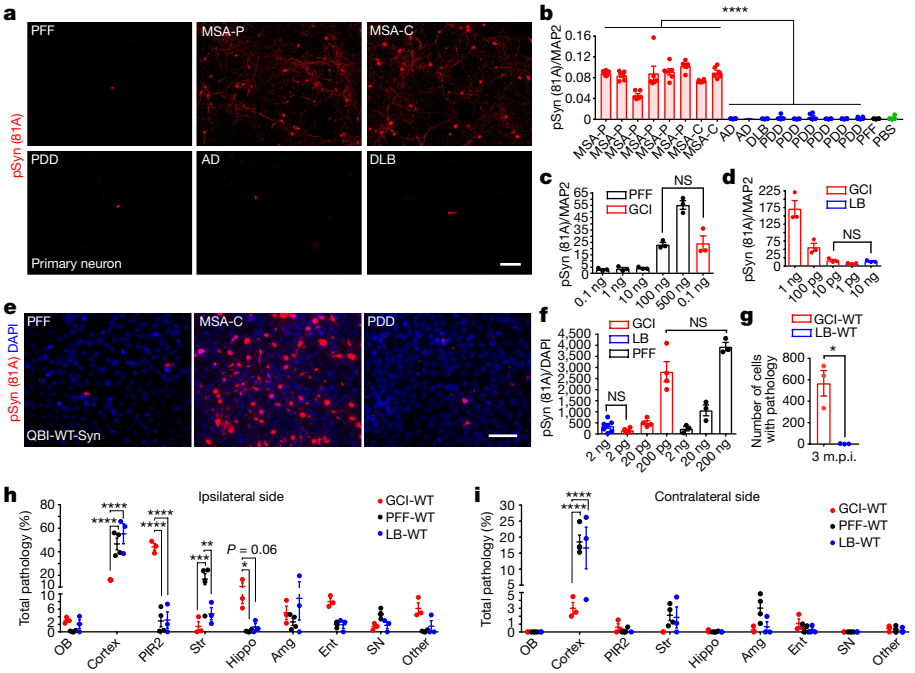

Fig. 2 | The seeding properties of GCI-α-Syn and LB-α-Syn do not show any cell-type preference. **a**, pS129 α-Syn induced by 1 ng of GCI-α-Syn, LB-α-Syn or PFFs in primary neurons (experiment repeated seven times). **b**, Quantification of α-Syn pathology for experiments in **a** (GCI, $n = 8$ different preparations, LB, $n = 9$ different preparations) (statistics: two-tailed unpaired t-test using the mean value of each case.). **c**, **d**, Quantification of pS129 α-Syn induced by various concentrations of PFFs, GCI-α-Syn or LB-α-Syn in neurons ($n = 3$ biological replicates) (statistics: adjusted with Bonferroni correction). **e**, pS129 α-Syn induced by 2 ng of GCI-α-Syn, LB-α-Syn or PFFs in QBI-WT-Syn cells (experiment repeated seven times). **f**, Quantification of pS129 α-Syn induced by various concentration of PFFs, GCI-α-Syn or LB-α-Syn in QBI-WT-Syn cells (LB, $n = 7$ (LB), 4 (GCI) or 3 (PFF) biological replicates) (statistics: adjusted with Bonferroni correction). **g**, Quantification of the number of cells with α-Syn pathology in wild-type mice inoculated with 50 ng of GCI-α-Syn or LB-α-Syn at three months post-injection (m.p.i.) ($n = 3$ mice). **h**, **i**, Quantification of the distribution of α-Syn pathology seeded by GCI-α-Syn (GCI-WT, $n = 3$ mice) or PFFs (PFF-WT, $n = 4$ mice) at three months post-injection and LB-α-Syn (LB-WT, $n = 3$ mice) at six months post-injection. Amg, amygdala; Cortex, cortex except pyramidal layer of piriform area (PIR2) and entorhinal cortex (Ent); Hippo, hippocampus; OB, olfactory bulb; SN, substantia nigra; Str, striatum. Results shown as mean ± s.e.m. Statistics shown in **h**, **i** are two-way ANOVA followed by Tukey's honest significant difference test. Scale bars: 100 μm (**a**), 50 μm (**e**). See Supplementary Table 5 for statistical details.

knockout mice, generating a new mouse line that expresses α-Syn only in oligodendrocytes (hereafter referred to as 'KOM2 mice') (Extended Data Fig. 6a, b).

KOM2 mice were unilaterally injected with GCI-α-Syn or LB-α-Syn into the thalamus (GCI-KOM2 and LB-KOM2 mice, respectively). At one month post-injection, although α-Syn inclusions appeared in the

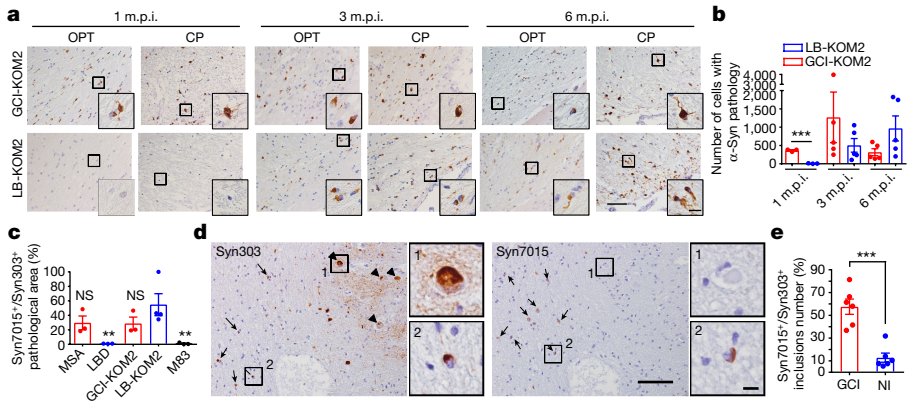

Fig. 3 | Oligodendrocyte environment generates the GCI-α-Syn strain. **a**, Syn506-positive α-Syn aggregates seeded by 18.75 ng of GCI-α-Syn or LB-α-Syn in KOM2 mice. OPT, optic tract; CP, cerebral peduncle (experiment repeated three times). **b**, Quantification of the number of oligodendrocytes with α-Syn pathology in injected KOM2 mice (one month post-injection, $n = 3$; three and six months post-injection, $n = 5$ mice) (statistics: adjusted with Bonferroni correction). **c**, Quantification of the ratio of area occupied by Syn7015-positive versus Syn303-positive α-Syn pathology in adjacent sections of brains from patients with MSA (MSA) or patients with Lewy body disease (LBD), injected KOM2 mouse brains or M83 transgenic mouse brains (GCI, $n = 3$ cases; LB, $n = 3$ cases; GCI-KOM2, LB-KOM2 and M83, $n = 4$ mice) (statistics: one-way ANOVA followed by Dunnett's post hoc test comparing each group with LB-KOM2). **d**, Adjacent sections of the medulla from an MSA case stained with Syn303 and Syn7015 (repeated with four cases). Arrows: GCIs; arrowheads: neuronal inclusions. **e**, Quantification of the ratio of Syn7015-positive versus Syn303-positive GCIs and neuronal inclusions (NI) on adjacent sections of brains from paients with MSA ($n = 6$ cases). Results shown as mean ± s.e.m. Scale bars: 50 μm (**a**); 12.5 μm (**a** insets); 100 μm (**d**); 10 μm (**d** insets). See Supplementary Table 5 for statistical details.

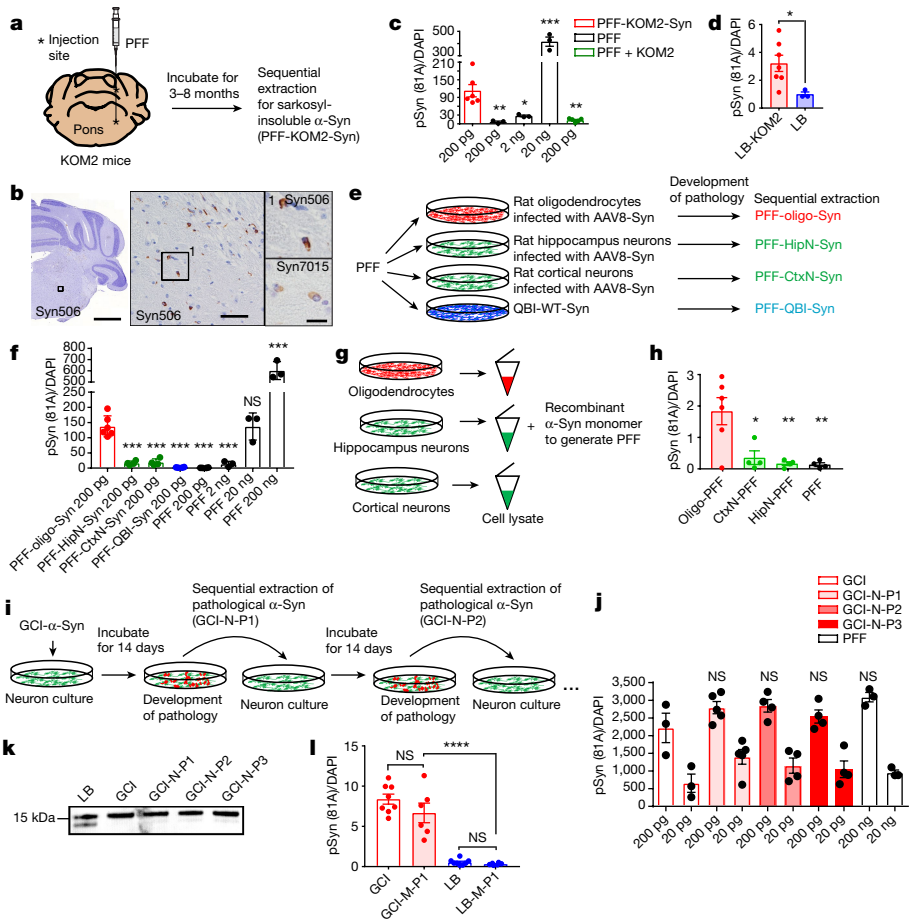

Fig. 4 | Oligodendrocytes convert misfolded α-Syn to a GCI-α-Syn-like strain but neurons could not convert GCI-α-Syn to a LB-α-Syn-like strain. a, Schematic for passaging PFFs in KOM2 mice. **b**, α-Syn pathology in PFF-injected KOM2 mice (experiment repeated three times). **c**, Quantification of pS129 α-Syn in QBI-WT-Syn cells seeded by PFFs, passaged PFFs (PFF-KOM2-Syn) or PFFs combined with insoluble fraction from uninjected KOM2 mice (PFF + KOM2) ($n = 6$ (PFF-KOM2-Syn), 3 (PFF) and 5 (PFF + KOM2) biological replicates). **d**, Quantification of pS129 α-Syn in QBI-WT-Syn cells seeded by equal amounts of LB-α-Syn or LB-α-Syn passaged in KOM2 mice (LB-KOM2) (LB, $n = 3$ biological replicates; LB-KOM2, $n = 7$ biological replicates). **e**, Schematic for passaging PFFs in various cells. **f**, Quantification of pS129 α-Syn in QBI-WT-Syn cells seeded by PFFs passaged in cells. PFF-oligo-Syn, PFF-HipN-Syn, PFF-CtxN-Syn and PFF-QBI-Syn refer to PFFs that have been passaged in oligodendrocytes, hippocampus neurons, cortical neurons and QBI-WT-Syn cells, respectively. ($n = 6$ (PFF-oligo-Syn), 4 (PFF-HipN-Syn, PFF-CtxN-Syn) and 3 (PFF) biological replicates). **g**, Schematic for generating α-Syn PFFs in cell lysates. **h**, Quantification of pS129 α-Syn in QBI-WT-Syn cells seeded by PFFs generated in oligodendrocyte lysate (oligo-PFF), cortex neuron lysate (CtxN-PFF), hippocampus neuron lysate (HipN-PFF) or with α-Syn monomer alone (PFF) ($n = 6$ (oligo-PFF) or 4 (CtxN-PFF, HipN-PFF, PFF) biological replicates). **i**, Schematic for passaging GCI-α-Syn in primary neurons. **j**, Quantification of pS129 α-Syn in QBI-WT-Syn cells seeded by α-Syn PFFs, GCI-α-Syn and GCI-α-Syn passaged in primary neurons ($n = 3$ (GCI, PFF), 4 (GCI-N-P2, GCI-N-P3) or 5 (GCI-N-P1) biological replicates). **k**, Proteinase K-digested LB-α-Syn, GCI-α-Syn, GCI-N-P1, GCI-N-P2 and GCI-N-P3 were immunoblotted with anti-α-Syn antibody (experiment repeated three times). **l**, Quantification of insoluble pS129 α-Syn in QBI-WT-Syn cells seeded by equal amounts of GCI-α-Syn, LB-α-Syn or GCI-α-Syn and LB-α-Syn passaged in M83 mice (GCI-M-P1 and LB-M-P1) ($n = 8$ (GCI, LB) or 6 (GCI-M-P1, LB-M-P1) biological replicates). Results shown as mean ± s.e.m. Statistics shown in **c**, **f**, **h** and **j** are one-way ANOVA followed by Dunnett's post hoc test comparing each group with PFF-KOM2-Syn (**c**), PFF-oligo-Syn (**f**), oligo-PFF (**h**) or GCI 200 pg (**j**). Statistics shown in **l** are one-way ANOVA followed by Tukey's multiple comparison's test. Scale bars: 1 mm (**b**); 50 μm (**b**, middle inset), 15 μm (**b**, right inset). For gel source data, see Supplementary Fig. 1. See Supplementary Table 5 for statistical details.

thalamus and fimbria of GCI-KOM2 mice, more abundant pathology was observed in the optic tract and cerebral peduncle; that is, sites distant from the injection site but highly enriched with oligodendrocytes, which suggests that α-Syn pathology spreads between oligodendrocytes. By contrast, few oligodendrocytes developed pathology in LB-KOM2 mice, demonstrating that GCI-α-Syn is more potent than LB-α-Syn. However, at three months post-injection—as the burden of pathology in GCI-KOM2 mice peaked—LB-KOM2 mice began to show substantial oligodendrocyte pathology. At six months post-injection, whereas the pathology in GCI-KOM2 mice declined precipitously, LB-KOM2 mice showed even more inclusions, which reached levels comparable to GCI-KOM2 mice at three months post-injection (Fig. 3a, b and Extended Data Fig. 7a–e). The presence of α-Syn pathology in oligodendrocytes and the phosphorylation of S129 were confirmed by immunostaining (Extended Data Fig. 7f, g). Mapping of α-Syn pathology in LB-KOM2 and GCI-KOM2 mice revealed a similar pattern (Extended Data Fig. 8). This delayed induction of α-Syn pathology in LB-KOM2 mice supports our hypothesis that LB-α-Syn is less potent than GCI-α-Syn, but that once initiated the subsequent propagation within oligodendrocytes results in the formation of a GCI-α-Syn-like strain.

Moreover, whereas Lewy bodies in the brains of patients with Parkinson's disease were not detected by Syn7015, the oligodendrocyte α-Syn pathologies induced by LB-α-Syn in KOM2 mice were Syn7015-positive (Fig. 3c and Extended Data Fig. 9a), suggesting that LB-α-Syn-induced oligodendrocyte pathology acquired properties of the GCI-α-Syn strain. Furthermore, detailed characterization of oligodendrocyte pathologies induced by GCI-α-Syn or LB-α-Syn

showed that they were indistinguishable, including co-localization with p62, partial co-localization with ubiquitin and association with reactive astrocytes (Extended Data Fig. 9b, c). Thus, LB-α-Syn can induce oligodendrocyte pathologies in the KOM2 mice that adopt properties of the GCI-α-Syn strain.

Both α-Syn neuronal inclusions and GCIs are present in the brains of patients with MSA, although neuronal inclusions are uncommon. We hypothesized that if the oligodendrocyte environment generates the GCI-α-Syn strain, neuronal inclusions in brains from paients with MSA would resemble Lewy bodies in brains from patients with Parkinson's disease. To test this, adjacent sections from six cases of MSA with neuronal inclusions in the medulla or hippocampus were immunostained with Syn7015 and Syn303. Syn7015 preferentially stained GCIs over neuronal inclusions (Fig. 3d, e), demonstrating that MSA neuronal inclusions are similar to Parkinson's disease Lewy bodies. Furthermore, Syn7015 also failed to detect neuronal inclusions in other brain regions—such as the substantia nigra and cortex—in additional cases of MSA (Extended Data Fig. 9d), which also provides support for our hypothesis.

To test our hypothesis further, we injected human α-Syn PFFs into the pons and cerebellum of KOM2 mice (Fig. 4a, b). Then, the induced pathological α-Syn (PFF-KOM2-Syn) was recovered by sequential extraction. Notably, PFF-KOM2-Syn was much more potent than the PFFs themselves in inducing α-Syn pathology (Fig. 4c and Extended Data Fig. 10a). By contrast, mixing PFFs with the sarkosyl-insoluble fraction from uninjected KOM2 mice only slightly increased the potency (Fig. 4c). A similar phenomenon was observed when passaging LB-α-Syn in KOM2 mice (Fig. 4d). To test whether this effect of the cellular milieu is unique to oligodendrocytes, PFFs were added to different cell types including oligodendrocytes, hippocampal and cortical neurons, and QBI-WT-Syn cells. After the induction of α-Syn pathology, sarkosyl-insoluble α-Syn was prepared from these cells (Fig. 4e). PFFs passaged through oligodendrocytes were more potent than PFFs passaged through other cell types (Fig. 4f and Extended Data Fig. 10b–d). Taken together, these results clearly demonstrate that the oligodendrocyte environment leads to the generation of the GCI-α-Syn strain.

To test whether the generation of the GCI-α-Syn strain depends on cell structures or specific 'factors', we prepared cell lysates from primary oligodendrocytes and neurons in which cell structures were disrupted but cell factors were preserved. We incubated each lysate with an equal amount of α-Syn monomer to generate α-Syn PFFs (Fig. 4g). PFFs generated in oligodendrocyte lysates were able to induce several-fold more pathology compared with PFFs generated in neuron lysates or with α-Syn monomers alone, supporting the hypothesis that the generation of the GCI-α-Syn strain relies on specific factors in oligodendrocytes (Fig. 4h).

Lastly, we asked whether the neuronal environment could convert the GCI-α-Syn strain to the LB-α-Syn strain. Primary mouse neurons were treated with GCI-α-Syn, and the induced α-Syn pathology was enriched by sequential extraction (pathological α-Syn labelled GCI-N-P1, GCI-N-P2 and GCI-N-P3 over three rounds of passaging) (Fig. 4i). Using enzyme-linked immunosorbent assays (ELISAs) that detect only human α-Syn or both human and mouse α-Syn, we estimated that majority (>99.7%) of pathological α-Syn in GCI-N-P1 was derived through recruitment of mouse α-Syn (Supplementary Table 3). GCI-N-P1 was as potent as GCI-α-Syn (Fig. 4j). Furthermore, the GCI-α-Syn strain was repetitively passaged in neurons such that even after three rounds of passaging GCI-N-P3 still maintained the marked activity of the GCI-α-Syn strain (Fig. 4j and Extended Data Fig. 10e–g). Proteinase K digestion revealed that after passaging in neurons, the GCI-α-Syn conformation was maintained (Fig. 4k). Furthermore, when both GCI-α-Syn and LB-α-Syn were passaged in M83 mice expressing mutant human (A53T) α-Syn[22], their different seeding properties were maintained (Fig. 4l). Thus, we conclude that the GCI-α-Syn strain can be maintained in a neuronal milieu. Combined with the observation that neuronal inclusions in MSA are similar to LB-α-Syn, our data suggest that GCI-α-Syn rarely transmits from oligodendrocytes to neurons in MSA brains, although we cannot exclude the possibility that GCI-α-Syn transmits to neurons, but that these neurons died.

Because LB-α-Syn could induce α-Syn pathology in oligodendrocytes expressing α-Syn in vitro and in vivo, the lack of GCIs in Lewy body diseases is unlikely to be due to the strain properties of LB-α-Syn, but might be attributable to the lack of α-Syn in oligodendrocytes[23]. The source of α-Syn in oligodendrocytes in MSA is still unclear. Two hypotheses have previously been proposed: (1) oligodendrocytes pathologically overexpress α-Syn in MSA[24] and (2) oligodendrocytes take up α-Syn from neurons[25]. GCI-α-Syn also could not induce α-Syn pathology in oligodendrocytes cultured in medium with high concentration of α-Syn monomer (data not shown), suggesting that internalization of exogenous α-Syn from the environment might be insufficient for GCI formation in oligodendrocytes.

Online content

Any Methods, including any statements of data availability and Nature Research reporting summaries, along with any additional references and Source Data files, are available in the online version of the paper at https://doi.org/10.1038/s41586-018-0104-4.

Received: 2 August 2017; Accepted: 6 April 2018;
Published online 9 May 2018.

1. Lippa, C. F. et al. Lewy bodies contain altered α-synuclein in brains of many familial Alzheimer's disease patients with mutations in presenilin and amyloid precursor protein genes. *Am. J. Pathol.* **153**, 1365–1370 (1998).
2. Spillantini, M. G. et al. α-Synuclein in Lewy bodies. *Nature* **388**, 839–840 (1997).
3. Tu, P. H. et al. Glial cytoplasmic inclusions in white matter oligodendrocytes of multiple system atrophy brains contain insoluble α-synuclein. *Ann. Neurol.* **44**, 415–422 (1998).
4. Bousset, L. et al. Structural and functional characterization of two α-synuclein strains. *Nat. Commun.* **4**, 2575 (2013).
5. Guo, J. L. et al. Distinct α-synuclein strains differentially promote tau inclusions in neurons. *Cell* **154**, 103–117 (2013).
6. Peelaerts, W. et al. α-Synuclein strains cause distinct synucleinopathies after local and systemic administration. *Nature* **522**, 340–344 (2015).
7. Prusiner, S. B. et al. Evidence for α-synuclein prions causing multiple system atrophy in humans with parkinsonism. *Proc. Natl Acad. Sci. USA* **112**, E5308–E5317 (2015).
8. Woerman, A. L. et al. Propagation of prions causing synucleinopathies in cultured cells. *Proc. Natl Acad. Sci. USA* **112**, E4949–E4958 (2015).
9. Fanciulli, A. & Wenning, G. K. Multiple-system atrophy. *N. Engl. J. Med.* **372**, 249–263 (2015).
10. Koga, S. & Dickson, D. W. Recent advances in neuropathology, biomarkers and therapeutic approach of multiple system atrophy. *J. Neurol. Neurosurg. Psychiatry* **89**, 175–184 (2018).
11. Fujiwara, H. et al. α-Synuclein is phosphorylated in synucleinopathy lesions. *Nat. Cell Biol.* **4**, 160–164 (2002).
12. Gorbatyuk, O. S. et al. The phosphorylation state of Ser-129 in human α-synuclein determines neurodegeneration in a rat model of Parkinson disease. *Proc. Natl Acad. Sci. USA* **105**, 763–768 (2008).
13. Covell, D. J. et al. Novel conformation-selective alpha-synuclein antibodies raised against different *in vitro* fibril forms show distinct patterns of Lewy pathology in Parkinson's disease. *Neuropathol. Appl. Neurobiol.* **43**, 604–620 (2017).
14. Duda, J. E., Giasson, B. I., Mabon, M. E., Lee, V. M. & Trojanowski, J. Q. Novel antibodies to synuclein show abundant striatal pathology in Lewy body diseases. *Ann. Neurol.* **52**, 205–210 (2002).
15. Irwin, D. J. et al. Neuropathologic substrates of Parkinson disease dementia. *Ann. Neurol.* **72**, 587–598 (2012).
16. Montine, T. J. et al. Multisite assessment of NIA-AA guidelines for the neuropathologic evaluation of Alzheimer's disease. *Alzheimers Dement.* **12**, 164–169 (2016).
17. Volpicelli-Daley, L. A. et al. Exogenous α-synuclein fibrils induce Lewy body pathology leading to synaptic dysfunction and neuron death. *Neuron* **72**, 57–71 (2011).
18. Luk, K. C. et al. Exogenous α-synuclein fibrils seed the formation of Lewy body-like intracellular inclusions in cultured cells. *Proc. Natl Acad. Sci. USA* **106**, 20051–20056 (2009).
19. Karpowicz, R. J. Jr et al. Selective imaging of internalized proteopathic α-synuclein seeds in primary neurons reveals mechanistic insight into transmission of synucleinopathies. *J. Biol. Chem.* **292**, 13482–13497 (2017).
20. Luk, K. C. et al. Pathological α-synuclein transmission initiates Parkinson-like neurodegeneration in nontransgenic mice. *Science* **338**, 949–953 (2012).
21. Yazawa, I. et al. Mouse model of multiple system atrophy α-synuclein expression in oligodendrocytes causes glial and neuronal degeneration. *Neuron* **45**, 847–859 (2005).

22. Giasson, B. I. et al. Neuronal α-synucleinopathy with severe movement disorder in mice expressing A53T human α-synuclein. *Neuron* **34**, 521–533 (2002).
23. Miller, D. W. et al. Absence of α-synuclein mRNA expression in normal and multiple system atrophy oligodendroglia. *J. Neural Transm. (Vienna)* **112**, 1613–1624 (2005).
24. Asi, Y. T. et al. Alpha-synuclein mRNA expression in oligodendrocytes in MSA. *Glia* **62**, 964–970 (2014).
25. Reyes, J. F. et al. Alpha-synuclein transfers from neurons to oligodendrocytes. *Glia* **62**, 387–398 (2014).

Acknowledgements We thank K. Brunden and J. Guo for critical reading of the manuscript; S. Xie for helping with statistics; L. Kwong and Y. Xu for helping with brain extraction; D. Riddle for providing primary neurons; L. Romero for helping with quantification; L. Changolkar for helping with ELISA and all the other members of the Center for Neurodegenerative Disease Research for their support; and J. Grinspan and C. Richter-Landsberg for advice on culturing oligodendrocytes. The anti-PLP antibody was provided by J. Grinspan. This work was supported by NIH/NINDS Udall Center grant NS53488, the Ofer Nimerovsky Family Fund, the Jeff and Anne Keefer Fund and the MSA Coalition Global Seed Grant.

Reviewer information *Nature* thanks T. Baron and the other anonymous reviewer(s) for their contribution to the peer review of this work.

Author contributions C.P. designed and performed the experiments, analysed the data and wrote the manuscript. R.J.G., C.M. and M.F.O. performed the animal experiments and did quantification analysis. R.J.G. also performed α-Syn ELISA and biochemical analysis. D.J.C. generated the Syn9027 and Syn7015 antibodies and α-Syn PFFs. A.S. generated the KOM2 mice and assisted in stereotaxic injections. J.L.R. scored stained human brain sections. B.Z., R.J.G. and M.F.O. performed stereotaxic injections. R.M.P. performed cell culture experiments. K.C.L performed experiments and reviewed the manuscript. J.Q.T. supervised the study and reviewed the manuscript. V.M.-Y.L. supervised the study, interpreted the data and wrote the manuscript.

Competing interests The authors declare no competing interests.

Additional information
Extended data is available for this paper at https://doi.org/10.1038/s41586-018-0104-4.
Supplementary information is available for this paper at https://doi.org/10.1038/s41586-018-0104-4.
Reprints and permissions information is available at http://www.nature.com/reprints.
Correspondence and requests for materials should be addressed to V.M.-Y.L.
Publisher's note: Springer Nature remains neutral with regard to jurisdictional claims in published maps and institutional affiliations.

METHODS

No statistical methods were used to predetermine sample size. The investigators were blinded to allocation during all quantification experiments involving manual counting.

Recombinant α-Syn purification and in vitro fibrillization. Full-length human and mouse α-Syn (1–140) proteins were expressed in BL21 (DE3) RIL cells and purified as previously described[26]. Fibrillization was conducted by diluting recombinant α-syn to 5 mg/ml in sterile Dulbecco's PBS (Cellgro, Mediatech; pH adjusted to 7.0) followed by incubating this recombinant α-Syn at 37 °C with constant agitation at 1,000 r.p.m. for 7 days. Successful α-Syn fibrillization was verified by sedimentation test and thioflavin T-binding assay as described[27].

Preparation of sarkosyl-insoluble fractions from disease and control brains. All human brain tissues are from the CNDR brain bank[28]. Preparations of the sarkosyl-insoluble fraction were performed as previously described[5] and outlined in Extended Data Fig. 1a. In brief, brain regions with abundant α-Syn inclusions from patients with MSA, PDD, DLB or AD were identified by post mortem histological examination[15]. The brains of patients with Alzheimer's disease were selected for the presence of abundant Lewy bodies in addition to plaques and tangles. Frozen brain tissues from the identified regions were homogenized in high-salt (HS) buffer (50 mM Tris-HCl pH 7.4, 750 mM NaCl, 10 mM NaF, 5 mM EDTA) with protease and protein phosphatase inhibitors, incubated on ice for 20 min and centrifuged at 100,000 *g* for 30 min. The pellets were then re-extracted with HS buffer, followed by sequential extractions with 1% Triton X-100-containing HS buffer and 1% Triton X-100-containing HS buffer with 30% sucrose. The pellets were then re-suspended and homogenized in 1% sarkosyl-containing HS buffer, rotated at 4 °C overnight and centrifuged at 100,000 *g* for 30 min. The resulting sarkosyl-insoluble pellets were washed once with Dulbecco's PBS and re-suspended in Dulbecco's PBS by brief sonication (QSonica Microson XL-2000; 20 pulses; setting 2; 0.5 s per pulse). This suspension was termed the 'sarkosyl-insoluble fraction', which contained pathological α-Syn and was used for the cellular and in vivo assays described in this Letter. The amount of α-Syn, tau, Aβ 40 and Aβ 42 in the sarkosyl-insoluble fractions was determined by sandwich ELISAs (see 'Sandwich ELISA') and the protein concentrations were examined by bicinchoninic acid assay. Proteinase K, trypsin and thermolysin digestion was performed as previously described[5].

Sandwich ELISA. The concentrations of tau, Aβ 1–40 and Aβ 1–42 in the sarkosyl-insoluble fraction of human brain extractions were measured using sandwich ELISA as previously described[29,30], with the following combinations of capture and reporting antibodies: Tau5/BT2^{+}HT7 for tau, Ban50/BA27 for Aβ 1–40, Ban50/BC05 for Aβ 1–42.

To measure the concentration of α-Syn, 384-well Nunc Maxisorp clear plates were coated with 100 ng (30 μl per well) Syn9027, a MAb to α-Syn, in Takeda buffer and incubated overnight at 4 °C. The plates were washed 4× with PBS containing 1% Tween 20 (PBS-T), and blocked using Block Ace solution (90 μl per well) (AbD Serotec) overnight at 4 °C. Then, the plates were incubated with brain lysates at 4 °C overnight using recombinant α-Syn monomer as standards. The plates were then washed with PBS-T and a rabbit monoclonal anti-α-Syn antibody, MJF-R1 (1:1,000, 30 μl per well) was added to each well and incubated at 4 °C overnight. After washing, goat-anti-rabbit-IgG conjugated to horse radish peroxidase (Cell Signaling Technology, 1:15,000, 30 μl per well) was added to the plates followed by incubation for 2 h at room temperature. Following another wash, the plates were developed for 10–15 min using 1-Step Ultra TMB-ELISA substrate solution (Fisher Scientific, 30 μl per well), the reaction was quenched using 10% phosphoric acid (30 μl per well) and plates were read at 450 nm on a Molecular Devices Spectramax M5 plate reader.

Cell cultures. Primary mouse neurons were prepared from the hippocampus of embryonic day (E) 15–E17 CD1 mouse embryos as previously described[27]. PFFs and sarkosyl-insoluble α-Syn fractions were diluted in Dulbecco's PBS (without Mg^{2+} or Ca^{2+}) and sonicated (QSonica Microson XL-2000; 60 pulses; setting 1.5; 0.5 s per pulse). Neurons were then treated with PBS, sonicated PFFs or the α-Syn sarkosyl-insoluble fractions at 10 days in vitro (DIV) and collected for immunocytochemistry at 14 days post-treatment. To passage GCIs in primary neurons, five million neurons were plated per 10 cm dish, treated with 30 ng of sonicated GCI-α-Syn at DIV 10 and collected at DIV 24 by sequential extraction with the same protocol as described for human brain, except that HS buffer (50 mM Tris-HCl pH 7.4, 750 mM NaCl, 10 mM NaF, 5 mM EDTA) containing 1% Triton-100 was used in the initial extraction. The amount of total α-Syn in the sarkosyl-insoluble fractions was determined by sandwich ELISA with antibodies against both mouse and human α-Syn (Syn9027 and HuA) and the amount of human α-Syn was examined by sandwich ELISA using MJF-R1, which recognizes only human α-Syn, as the reporter antibody. Proteinase K digestion was performed as above described for GCI-α-Syn and LB-α-Syn. Treatment of primary neurons with chloroquine was performed as previously described[19].

Primary oligodendrocytes were prepared from the cortex of neonatal Sprague Dawley rats (Charles River Laboratories) as previously described[31]. In brief, oligodendrocyte progenitor cells were purified from mixed glial culture by mechanical shaking. The purified oligodendrocyte progenitor cells were plated on poly-L-lysine-coated coverslips and infected with AAV8-α-Syn-mCherry or AAV8-α-Syn three days after plating. Then, differentiation was induced three days after infection by culturing oligodendrocyte progenitor cells in the differentiation medium. Treatment with sonicated α-Syn PFF and sarkosyl-insoluble fractions was performed three days after differentiation as described above. Treated oligodendrocytes were collected for immunocytochemistry at 14 days post-treatment. To evaluate the purity of the oligodendrocyte culture, three independent cultures were stained with various cell markers for astrocytes (glial fibrillary acidic protein, GFAP), microglial (Iba1), neuron (NeuN) and oligodendrocytes (Olig2) at DIV 3, DIV 9 and DIV 23. At least three different 20× images were randomly taken for each coverslip and at least three coverslips were analysed for each time point for each cell marker.

To passage PFF in primary oligodendrocytes, two million oligodendrocyte progenitor cells were plated in a 10-cm dish, infected with AAV8-Syn to express human α-Syn, differentiated and treated with sonicated α-Syn PFFs as described above. Cells were collected at 14 days after treatment by sequential extraction with the same protocol as described for primary mouse neurons. The amount of total α-Syn in the sarkosyl-insoluble fractions was determined by sandwich ELISA with three different combinations of capture and reporting antibodies (Syn9027 + HuA, Syn9027 + MJF-R1 and HuA + Syn211).

The culture of QBI-WT-Syn cells and treatment with misfolded α-Syn were performed as previously described[18]. To induce α-Syn pathology in QBI-WT-Syn cells, one million QBI-WT-Syn cells were plated in a 6-cm dish and treated with PFFs two days later. Cells were collected at three days post-treatment by sequential extraction with the same protocol as described for primary mouse neurons. The amount of total α-Syn in the sarkosyl-insoluble fractions was determined by sandwich ELISA with three different combinations of capture and reporting antibodies (Syn9027 + HuA, Syn9027 + MJF-R1 and HuA + Syn211).

Primary hippocampus and cortical neurons of Sprague Dawley rats were generated from the Neuron Culture Service Center at University of Pennsylvania. To passage PFFs in primary rat neurons, 1.2 million hippocampus or cortical neurons were plated in a 6-cm dish, infected with AAV8-α-Syn at DIV 3 to express human α-Syn and treated with PFFs at DIV 6 as described above. Cells were collected at 14 days post-treatment by sequential extraction with the same protocol as described for primary mouse neurons. The amount of total α-Syn in the sarkosyl-insoluble fractions was determined by sandwich ELISA with three different combinations of capture and reporting antibodies (Syn9027 + HuA, Syn9027 + MJF-R1 and HuA + Syn211).

Stereotaxic injection of sarkosyl-insoluble fraction of pathological α-Syn and α-Syn PFFs. Sarkosyl-insoluble fractions from diseased brains were diluted in sterile Dulbecco's PBS to reach the same concentration of α-Syn in the samples and sonicated as described above. Two-to-three-month-old C57BL6/C3H wild-type mice or 3–4-month-old KOM2 mice were anaesthetized with ketamine hydrochloride (100 mg/kg), xylazine (10 mg/kg) and acepromazine (0.1 mg/kg). For wild-type mice, 50 ng of sarkosyl-insoluble pathological α-Syn from two different MSA brains and one brain of a patient with PDD ('PDD brain') or 6.25 μg mouse PFFs in 2.5 μl Dulbecco's PBS was stereotaxically injected into the dorsal striatum (coordinates: 0.2 mm relative to bregma, +2.0 mm from midline, +3.2 mm beneath the surface of skull) with 10-μl syringes (Hamilton) at a rate of 0.4 μl per min. For KOM2 mice, 18.75 ng of pathological α-Syn from three different MSA brains, two different PDD brains and one brain of a patient with DLB ('DLB brain') in 2.5 μl Dulbecco's PBS was stereotaxically injected into the thalamus, an area of relatively high oligodendrocyte α-Syn expression in these mice (coordinates: −2.5 mm relative to bregma, +2.0 mm from midline, +3.4 mm beneath the surface of skull) at a rate of 0.4 μl per min. Animals were then euthanized at 1, 3 and 6 month post-injection.

To passage PFFs in KOM2 mice, 5 mg/ml PFFs were sonicated as described above and stereotaxically injected into the pons and cerebellum of the KOM2 mice (coordinates: −5.45 mm relative to bregma, +1.1 mm from midline, +5 mm beneath the surface of skull for pons and +2.6 mm for cerebellum). PFFs were injected into pons (1 μl of PFFs) and cerebellum (1.5 μl) at a rate of 0.1 μl per min. Mice were euthanized at 3–8 months post-injection and the pons and cerebellum were either processed for histological studies or frozen for sequential extraction. Sequential extractions were performed with the same protocol as described for human brain except that the two rounds of extraction of HS buffer were omitted and the extraction began with 1% Triton, containing HS buffer. The amount of pathological α-Syn in the sarkosyl-insoluble fraction was examined by sandwich ELISAs with two different combinations of capture and reporting antibodies (9027 + MJF-R1 and Syn211 + HuA). To passage LB-α-Syn in KOM2, 2.5 μl of LB-α-Syn at the concentration of 7.52–15.87 ng/μl was injected into the pons and cerebellum or the thalamus of KOM2 mice. Mice were euthanized at 3–8 months post-injection and the brains were sequentially extracted and analysed in the same

way as PFF-injected KOM2 mice. To passage LB-α-Syn and GCI-α-Syn in M83 mice, 2.5 μl of GCI-α-Syn or LB-α-Syn at the concentration of 7.52 ng/μl was injected bilaterally into the striatum of M83 mice. Mice were euthanized at one month post-injection and the brains were sequentially extracted and analysed in the same way as PFF-injected KOM2 mice.

Immunohistochemistry. For histological studies, animals were transcardially perfused with PBS and the brain and spinal cord were removed and fixed in 70% ethanol (in 150 mM NaCl, pH 7.4) overnight before being processed for paraffin embedding. Immunohistochemistry was performed on 6-μm thick sections as previously described[32, 33]. The names and dilutions of the primary antibodies used here are shown in Supplementary Table 4. Stained sections were digitized using a Perkin Elmer Lamina scanner at 20× magnification. For quantitative analysis of α-Syn pathology in the mouse brain, Syn506-stained sections spanning the entire mouse brain at ~120-μm intervals were counted manually for the total number of cells with α-Syn positive inclusions. The semiquantitative heat maps were generated as previously described[34] using Syn506-stained slides. To quantify the spreading of pathological α-Syn in wild-type mice, representative Syn506-stained brain sections at bregma 4.28, 2.10, 0.98, −0.22, −1.22, −2.18, −2.92, −3.52 and −4.48 mm were counted manually for the number of cells with α-Syn pathology in each brain region. For GCI-WT and PFF-WT mice, 1–3 brain sections at each bregma point have been quantified and the mean value of these 1–3 brain sections has been used for quantification. For LB-WT mice, because of the low amount of pathology, 3–13 brain sections at each bregma point have been quantified.

For the quantification of neuronal inclusions in cases of MSA, adjacent sections of medulla or hippocampus from six cases of MSA were stained with Syn7015 and Syn303. The stained sections were digitized and the number of neuronal inclusions labelled by each antibody was quantified manually for each inferior olivary nucleus in medulla and dentate gyrus in hippocampus. To quantify the number of stained GCIs, three to six 10× images were randomly sampled in the white matter region near each inferior olivary nucleus or dentate gyrus. The positions of these 10× images were digitally labelled by drawing lines on the boundaries, and the same 10× images were sampled on adjacent sections by copying these annotations using the digitized image, and the total number of GCIs labelled by Syn7015 or Syn303 in these sampled areas were counted manually.

To grade the α-Syn pathology revealed by Syn7015 or Syn303 immunohistochemistry in MSA and LB-spectrum α-synucleinopathies, adjacent sections of hippocampus, frontal cortex, substantia nigra, cerebellum or midbrain from three cases of AD, three cases of DLB, three cases of PDD, four cases of MSA-C and three cases of MSA-P (see Supplementary Table 1) were stained with Syn7015 and Syn303 and graded by experienced pathologists. To quantify the ratio of total amount of Syn7015-positive versus Syn303-positive GCI or Lewy body, the stained adjacent sections were digitized and the total area occupied by Syn7015-positive or Syn303-positive α-Syn inclusions was quantified using an automated threshold-based algorithm by HALO software (http://www.indicalab.com/halo/). Then, the ratios of total Syn7015-positive area versus Syn303-positive area were calculated. For the serial dilution of Syn7015 and Syn303, all the ratios were calculated against the area occupied by immunohistochemistry conducted with the highest concentration of Syn303 (45 ng ml).

Animals. Two-to-three-month-old C57BL6/C3H wild-type mice were purchased from the Jackson Laboratories (Bar Harbour). M2 mice expressing wild-type human α-Syn in oligodendrocytes under the control of CNP promoter have previously been described[21]. KOM2 mice were generated by crossing M2 mice with $Snca^{-/-}$ mice[35]. Three-to-four-month-old KOM2 mice have been used for the study. All breeding, housing, and experimental procedures were performed according to the NIH Guide for the Care and Use of Experimental Animals and approved by the University of Pennsylvania Institutional Animal Care and Use Committee (IACUC). Both male and female mice were used for this study. Mice were randomly assigned to each experimental group. Roughly equal numbers of male and female KOM2 mice have been used in each group. All the GCI-WT and LB-WT mice were female. All the three-months-post-injection PFF-WT mice were female. For the six-months-post-injection PFF-WT mice, three of them were male and one was female.

Immunocytochemistry and quantification. For regular immunocytochemistry, cells were fixed in 4% paraformaldehyde (PFA) for 15 min followed by permeabilization with 0.1% Triton X-100 for 15 min. To examine α-Syn aggregates, cells were fixed with 4% PFA containing 1% Triton X-100 for 15 min to remove soluble proteins. Fixed coverslips were blocked with 3% BSA and 3% FBS for 1 h at room temperature and incubated with specific primary antibodies (Supplementary Table 4) at 4 °C overnight followed by staining with secondary antibodies for 2 h at room temperature. After mounting with Fluoromount G with DAPI (eBioscience), coverslips were scanned on a Perkin Elmer Lamina scanner. The total amount of 81A signal, the total amount of MAP2 signals for neuronal cultures and the total number of DAPI-positive nuclei for oligodendrocytes and QBI-WT-Syn cells were quantified using Indica Labs HALO software. For cells cultured in 96-well plates, cells were incubated in DAPI solution after staining with secondary antibodies. Then, plates were scanned with In Cell Analyzer 2200 (GE Healthcare) and analysed using the accompanying software (In Cell Toolbox Analyzer).

Purification and depletion of α-Syn from the sarkosyl-insoluble fraction by immunoprecipitation. Control mouse IgG (Sigma) or Syn9027 MAb—an in-house-generated Mab against α-Syn (epitope aa130–140)—were coupled to tosyl-activated Dynabeads (Invitrogen) or NHS-activated magnetic beads (Thermo Scientific) following the manufacturer's instructions. For immunoprecipitation purification, sarkosyl-insoluble fractions from diseased brains were incubated with control IgG-coupled beads in Dulbecco's PBS and rotated at 4 °C overnight. The resulting supernatant was then incubated with Syn9027-coupled beads in a rotator at 4 °C overnight to capture α-Syn. The following day, the Syn9027 beads were washed 3 times with Dulbecco's PBS and incubated with 0.1 M ethanolamine (pH 11.5) for 3–7 min at 55 °C to elute the bound α-Syn, which was then neutralized immediately with 1 M Tris (pH 7.0) and the eluted samples were stored at −80 °C until use. For immunoprecipitation depletion, the sarkosyl-insoluble fractions from diseased brains were incubated with Syn9027-coupled beads at 4 °C overnight. The resulting supernatants were incubated with Syn9027 beads again for a second round of α-Syn depletion and the final supernatants were stored at −80 °C until use.

Evaluatuing α-Syn expression in KOM2 mice. Total proteins were extracted from KOM2 and wild-type mice by sonicating the brain in 1% Triton X-100-containing HS buffer with phosphatase and protease inhibitors, and centrifuging at 100,000*g* for 30 min at 4 °C. Protein concentration of the supernatant was determined by BCA assay and same amount of protein from each mouse was resolved on 12% Bis-Tris gel and immunoblotted with antibodies against total α-Syn, mouse α-Syn or β-tubulins.

Generation of PFFs in different cell lysates. Neuron and oligodendrocyte cell lysates were prepared by sonicating primary rat hippocampus or cortical neurons at DIV 12 and oligodendrocyte cultures at DIV 10–12 in Dulbecco's PBS. The protein concentrations of cell lysates were evaluated by BCA assay and adjust to 1.86 mg/ml. α-Syn monomer was added to these cell lysates at the final concentration of 500 μg/ml and shaken at 37 °C with constant agitation at 1,000 r.p.m. for 14 days.

Statistical analysis. Unless specified otherwise, a two-tailed unpaired Student's *t*-test was used for all the comparisons in the study, and differences with *P* values of less than 0.05 were considered significant. For each *t*-test, an *F* test was also performed to evaluate the differences in variances. If there was a significant difference in variances ($P < 0.05$ by *F* test), Welch's correction on *t*-test was performed. Multiple comparisons were adjusted with Bonferroni correction. Detailed information regarding statistical analyses is provided in Supplementary Table 5.

Reporting summary. Further information on experimental design is available in the Nature Research Reporting Summary linked to this paper.

Data availability. All data generated or analysed during this study are included in the Letter and its Supplementary Information.

26. Giasson, B. I., Murray, I. V., Trojanowski, J. Q. & Lee, V. M. A hydrophobic stretch of 12 amino acid residues in the middle of α-synuclein is essential for filament assembly. *J. Biol. Chem.* **276**, 2380–2386 (2001).
27. Volpicelli-Daley, L. A., Luk, K. C. & Lee, V. M. Addition of exogenous α-synuclein preformed fibrils to primary neuronal cultures to seed recruitment of endogenous α-synuclein to Lewy body and Lewy neurite-like aggregates. *Nat. Protocols* **9**, 2135–2146 (2014).
28. Toledo, J. B. et al. A platform for discovery: the University of Pennsylvania Integrated Neurodegenerative Disease Biobank. *Alzheimers Dement.* **10**, 477–484.e1 (2014).
29. Guo, J. L. & Lee, V. M. Seeding of normal Tau by pathological Tau conformers drives pathogenesis of Alzheimer-like tangles. *J. Biol. Chem.* **286**, 15317–15331 (2011).
30. Lee, E. B., Skovronsky, D. M., Abtahian, F., Doms, R. W. & Lee, V. M. Secretion and intracellular generation of truncated Aβ in β-site amyloid-β precursor protein-cleaving enzyme expressing human neurons. *J. Biol. Chem.* **278**, 4458–4466 (2003).
31. Richter-Landsberg, C. & Vollgraf, U. Mode of cell injury and death after hydrogen peroxide exposure in cultured oligodendroglia cells. *Exp. Cell Res.* **244**, 218–229 (1998).
32. Duda, J. E. et al. Immunohistochemical and biochemical studies demonstrate a distinct profile of α-Synuclein permutations in Multiple System Atrophy. *J. Neuropathol.* **59**, 830–841 (2000).
33. Luk, K. C. et al. Intracerebral inoculation of pathological α-synuclein initiates a rapidly progressive neurodegenerative α-syncleinopathy in mice. *J. Exp. Med.* **209**, 975–986 (2012).
34. Iba, M. et al. Synthetic tau fibrils mediate transmission of neurofibrillary tangles in a transgenic mouse model of Alzheimer's-like tauopathy. *J. Neurosci.* **33**, 1024–1037 (2013).
35. Abeliovich, A. et al. Mice lacking α-synuclein display functional deficits in the nigrostriatal dopamine system. *Neuron* **25**, 239–252 (2000).

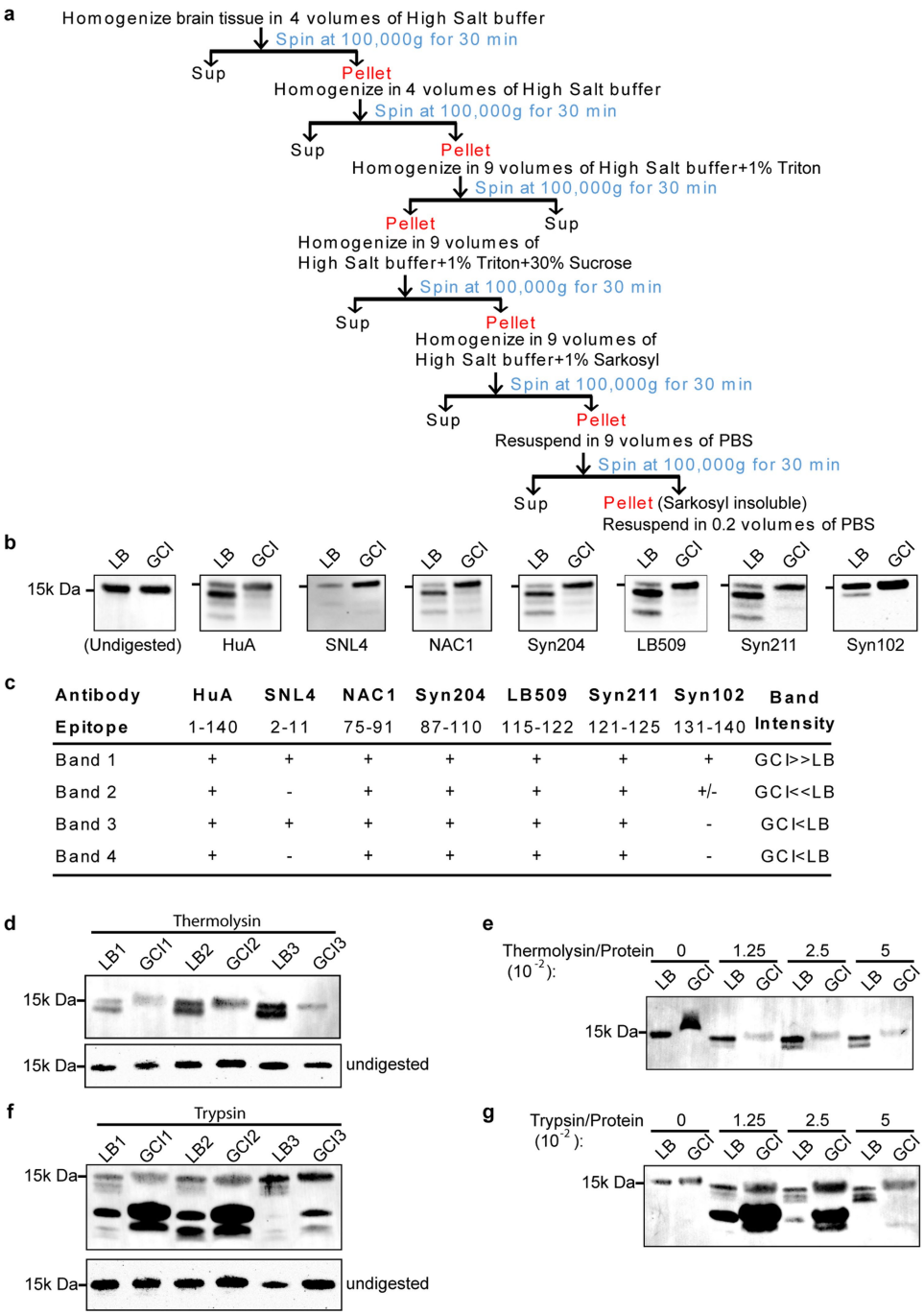

Antibody	HuA	SNL4	NAC1	Syn204	LB509	Syn211	Syn102	Band
Epitope	1-140	2-11	75-91	87-110	115-122	121-125	131-140	Intensity
Band 1	+	+	+	+	+	+	+	GCI>>LB
Band 2	+	-	+	+	+	+	+/-	GCI<<LB
Band 3	+	+	+	+	+	+	-	GCI<LB
Band 4	+	-	+	+	+	+	-	GCI<LB

Extended Data Fig. 1 | Biochemical analysis of GCI-α-Syn and LB-α-Syn. a, Schematic for sequential extraction of brains with α-synucleinopathy. Diseased brain samples were sequentially extracted with buffer of increasing extraction strengths (1% Triton X-100 followed by 1% sarkosyl) to remove soluble proteins. **b**, Proteinase K-digested GCI-α-Syn and LB-α-Syn were immunoblotted with a series of antibodies targeting specific domains of α-Syn that spanning the entire molecule. **c**, Summary of the results for experiments described in **b**. **d**, Thermolysin-digested and undigested sarkosyl-insoluble fractions from three cases of Lewy body disease (LB1–LB3) and three cases of MSA (GCI1–GCI3) were resolved on 12% Bis-Tris gel and immunoblotted with an antibody against α-Syn (Syn211). **e**, Sarkosyl-insoluble fractions from a pair of cases (one of Lewy body disease and one of MSA) were incubated with increasing concentrations of thermolysin (with a ratio of thermolysin to total protein that ranged from 1.25×10^{-2} to 5×10^{-2}) and immunoblotted with antibody against α-Syn (Syn211). Undigested fractions were loaded on the same gel. **f**, Trypsin-digested and undigested sarkosyl-insoluble fractions from three cases of Lewy body disease (LB1–LB3) and three cases of MSA (GCI1–GCI3) were resolved on 12% Bis-Tris gel and immunoblotted with an antibody against α-Syn (Syn211). **g**, Sarkosyl-insoluble fractions from a pair of cases (one of Lewy body disease and one of MSA) were incubated with increasing concentrations of trypsin (with the ratio of trypsin versus total protein range from 1.25×10^{-2} to 5×10^{-2}) and immunoblotted with an antibody against α-Syn (Syn211). Undigested fractions were loaded on the same gel. The experiments shown in **b** and **d**–**g** have been repeated three times with similar results. For gel source data, see Supplementary Fig. 1.

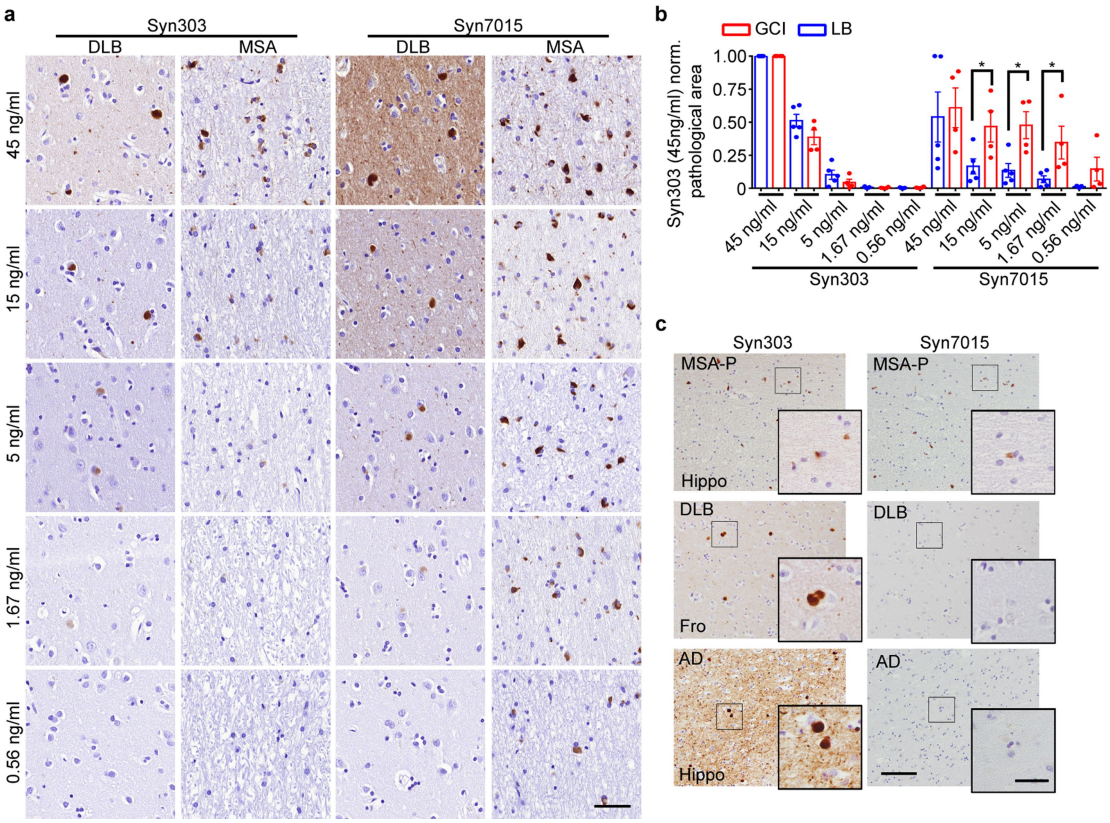

Extended Data Fig. 2 | Syn7015 preferentially recognizes GCIs over Lewy bodies. a, Immunohistochemistry using a series dilution of Syn303 or Syn7015 on serial sections of a DLB brain and a MSA brain. At 45 ng ml^{-1}, Syn7015 recognized both Lewy bodies and GCIs. At lower concentrations—particularly 1.67 ng ml^{-1} and 0.56 ng ml^{-1}—Syn7015 preferentially recognizes GCIs over Lewy bodies (repeated with four cases). **b**, Quantification of the area occupied by pathological α-Syn stained with serial dilutions of Syn7015 or Syn303 on serial sections of two cases of MSA-P, two cases of MSA-C, one case of AD, two cases of PDD and two cases of DLB. The results for each case are normalized to Syn303 staining at 45 ng ml^{-1} (GCI, $n = 4$ cases; LB, $n = 5$ cases). **c**, α-Syn pathology revealed by Syn303 or Syn7015 in adjacent sections from cases of Lewy body disease and MSA (repeated with seven cases). Results shown as mean ± s.e.m. *$P < 0.05$. Scale bar: 50 μm (**a**), 100 μm (**c**), 25 μm (**c** inset). See Supplementary Table 5 for statistical details.Source Data

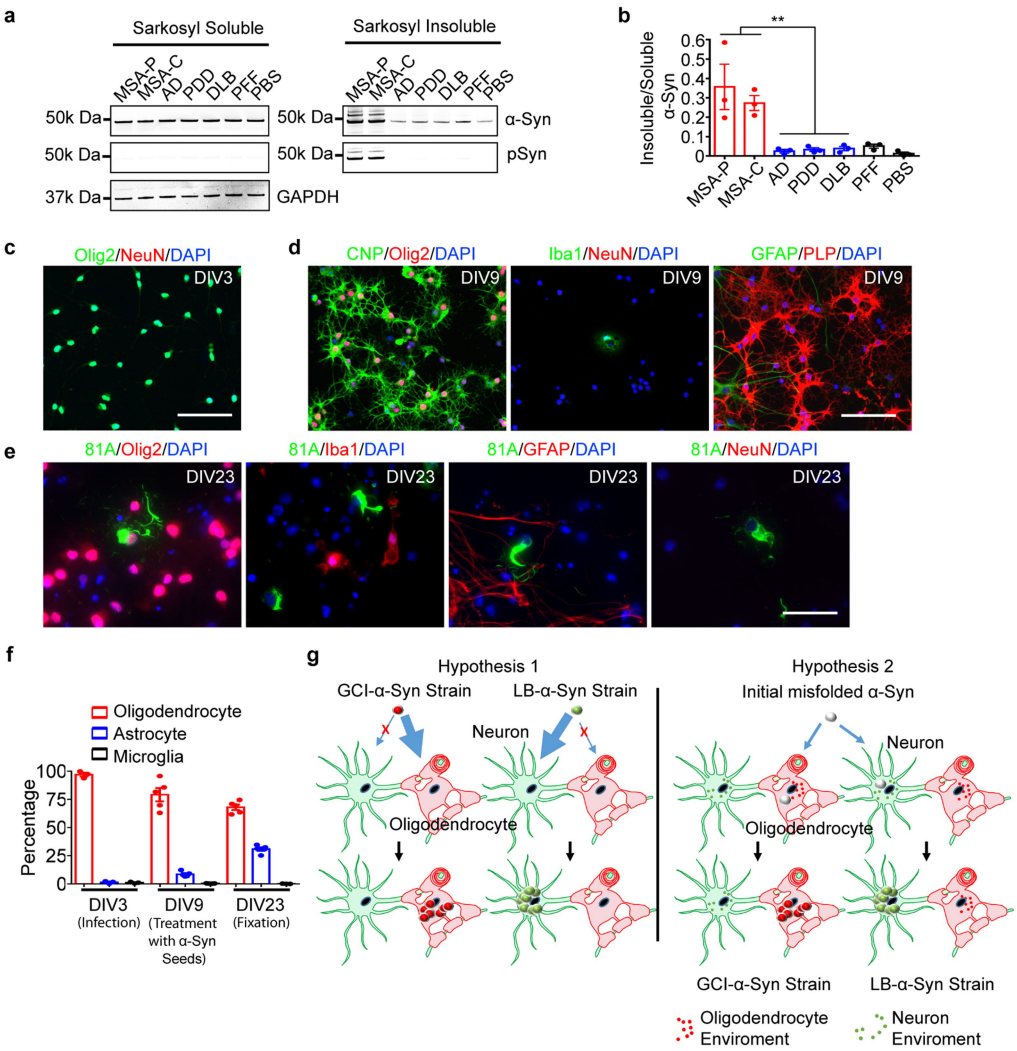

Extended Data Fig. 3 | GCI-α-Syn is more potent in inducing α-Syn pathology in primary oligodendrocytes. a, Oligodendrocytes treated with the same amount of GCI-α-Syn, LB-α-Syn or PFF were sequentially extracted with 1% Triton-X100 lysis buffer followed by 1% sarkosyl lysis buffer, which were combined together as the sarkosyl-soluble fraction. The sarkosyl-insoluble pellets were resuspended in Dulbecco's PBS by sonication. Both soluble and insoluble fractions were immunoblotted with an antibody against total or pS129 α-Syn. **b**, Densitometric quantification of insoluble versus soluble α-Syn for experiments described in **a** ($n = 3$ biological replicates). **c**, **d**, Primary oligodendrocyte cultures were immunostained with antibodies against various cell-type specific markers: CNP (oligodendrocytes), olig2 (oligodendrocytes), Iba1 (microglial cells), NeuN (neurons), GFAP (astrocytes), PLP (oligodendrocytes) at day in vitro 3 (DIV 3) (**c**) or DIV 9 (**d**). **e**, Insoluble phosphorylated α-Syn, induced in primary oligodendrocytes overexpressing α-Syn, was co-stained with antibodies against various cell-type specific markers, demonstrating that the cells with α-Syn pathology are oligodendrocytes. **f**, Percentage of different type of cells (oligodendrocytes, microglial cells and astrocytes) in oligodendrocyte culture, at DIV 3 (the time point of virus infection), DIV 9 (the time point for misfolded α-Syn treatment) and DIV 23 (the time point for fixation) ($n = 3$ (DIV3) or 5 (DIV 9, DIV 23) coverslips from three independent experiments). **g**, Working hypotheses regarding the different cell-type distributions of GCI-α-Syn and LB-α-Syn strains in diseased brains. Hypothesis 1 states that the unique properties of GCI-α-Syn and LB-α-Syn strains determine their different cell-type distributions. The GCI-α-Syn strain (represented by red spheres) is more efficient in inducing α-Syn pathology in oligodendrocytes, whereas the LB-α-Syn strain (green spheres) is more efficient in inducing α-Syn pathology in neurons. Hypothesis 2 states that GCI-α-Syn and LB-α-Syn strains do not have cell-type preferences and that they could both be initiated by the same misfolded α-Syn seeds (grey spheres), but that the different intracellular environments of neurons and oligodendrocytes convert these α-Syn seeds to different strains. Results shown as mean ± s.e.m. $^{**}P < 0.01$. Scale bars: 100 μm (**c**, **d**); 50 μm (**e**). The experiments shown in **a** and **c**–**e** have been repeated three times with similar results. See Supplementary Table 5 for statistical details. For gel source data, see Supplementary Fig. 1.Source Data

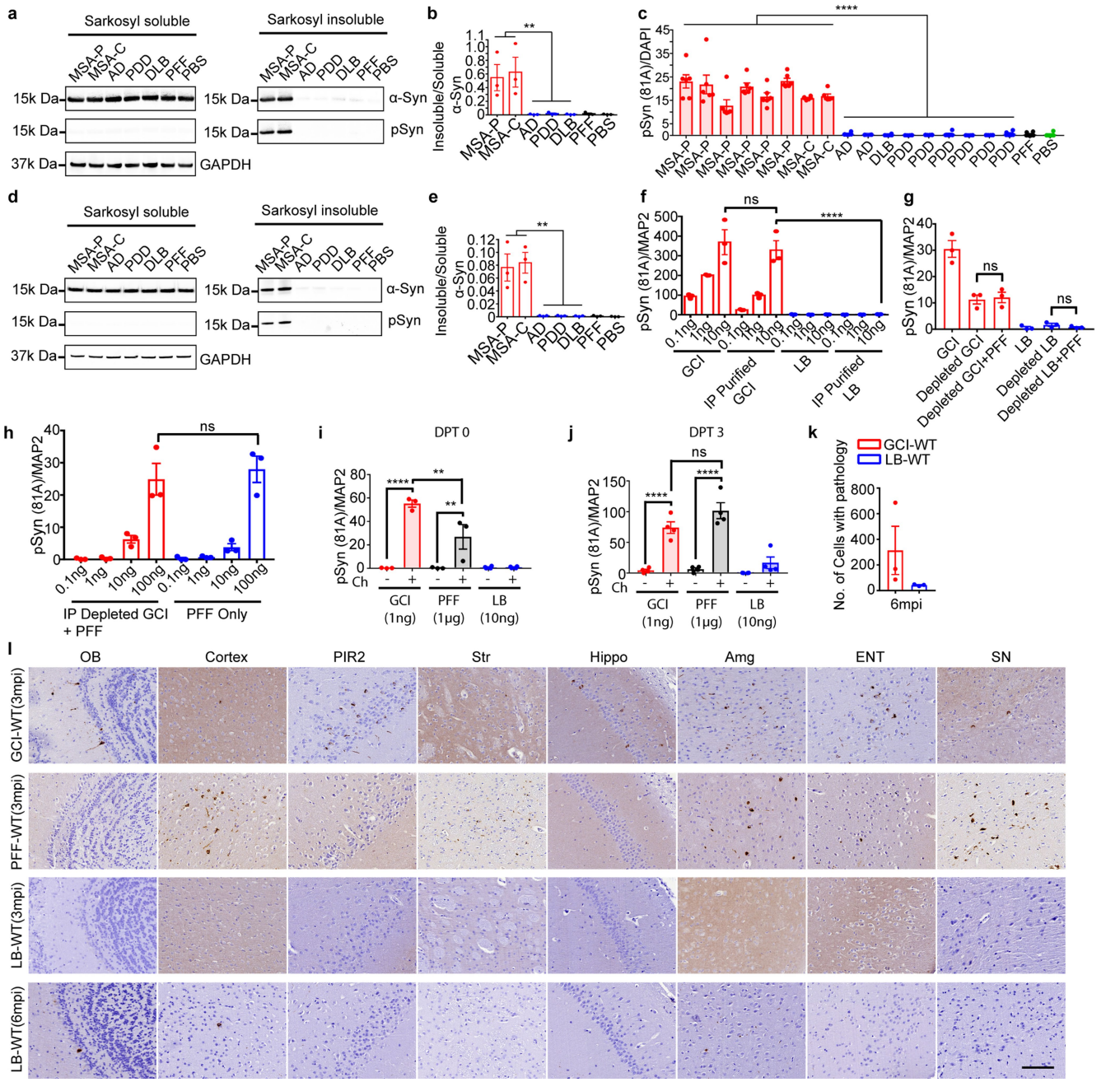

Extended Data Fig. 4 | See next page for caption.

Extended Data Fig. 4 | The seeding properties of GCI-α-Syn and LB-α-Syn do not show cell-type preference. a, Soluble and insoluble fractions from primary neurons treated with the same amount of GCI-α-Syn, LB-α-Syn or PFF were immunoblotted with antibodies against total or pS129 α-Syn. **b**, Densitometric quantification of insoluble versus soluble α-Syn for experiments described in **a** ($n = 3$ biological replicates). **c**, Quantification of phosphorylated α-Syn in QBI-WT-Syn cells induced by an equal amount of GCI-α-Syn (MSA-C, MSA-P), LB-α-Syn (PDD, DLB and AD) or PFFs (GCI, $n = 8$ different preparations; LB, $n = 9$ different preparations). **d**, Soluble and insoluble fractions from QBI-Syn-WT cells treated with the same amount of GCI-α-Syn, LB-α-Syn or PFF were immunoblotted with an antibody against total or pS129 α-Syn. **e**, Densitometric quantification of insoluble versus soluble α-Syn for experiments described in **d** ($n = 3$ biological replicates). **f**, Quantification of insoluble phosphorylated α-Syn in primary neurons induced by various concentrations of GCI-α-Syn and LB-α-Syn before or after immunoprecipitation purification ($n = 3$ independent experiments). **g**, Quantification of insoluble phosphorylated α-Syn in primary neurons incubated with (1) GCI-α-Syn and LB-α-Syn preparations; (2) the same preparations after immunoprecipitation depletion to remove α-Syn; and (3) the depleted preparation to which the same amount of α-Syn PFFs (1 ng) was added ($n = 3$ independent experiments). **h**, PFFs combined with the GCI-α-Syn preparation depleted of α-Syn behave similarly to α-Syn PFFs alone. Quantification of insoluble phosphorylated α-Syn in primary neurons seeded by PFFs alone or PFFs combined with depleted GCI preparation (the amount of pathology induced by immunoprecipitation-depleted GCI preparation alone has been subtracted) ($n = 3$ independent experiments). **i**, **j**, Primary neuron were treated with GCI-α-Syn, LB-α-Syn or PFF and incubated with chloroquine (Ch) at the day of misfolded α-Syn treatment ('DPT0') or three days post-treatment (DPT3). The amount of insoluble phosphorylated α-Syn was quantified three days after chloroquine treatment ($n = 3$ (DPT0-GCI and PFF) or 4 (DPT0-LB, DPT3) independent experiments). **k**, Quantification of the number of cells with α-Syn pathology in wild-type mice inoculated with 50 ng of GCI-α-Syn or LB-α-Syn at six months post-injection. **l**, Representative photomicrographs of α-Syn pathology (stained by Syn506) in multiple brain regions ipsilateral to the injection site in GCI-α-Syn-, PFF- and LB-α-Syn-injected wild-type mice. Cortex, motor cortex; ENT, entorhinal cortex. Results shown as mean ± s.e.m. $*P < 0.05$; $**P < 0.01$; $****P < 0.0001$; ns, not significant. Statistics shown in **c** represent two-tailed, unpaired *t*-test using the mean value of each case. Statistics shown in **f** represent one-way Anova with Tukey's multiple comparison test. Statistics shown in **g**, **h** are two-tailed, unpaired *t*-test adjusted with Bonferroni correction for multiple comparison. Statistics shown in **i**, **j** are two-way ANOVA, with Sidak's multiple comparisons test. The experiments in **a**, **d** and **l** have been repeated three times with similar results. Scale bar: 100 μm. See Supplementary Table 5 for statistical details. For gel source data, see Supplementary Fig. 1.Source Data

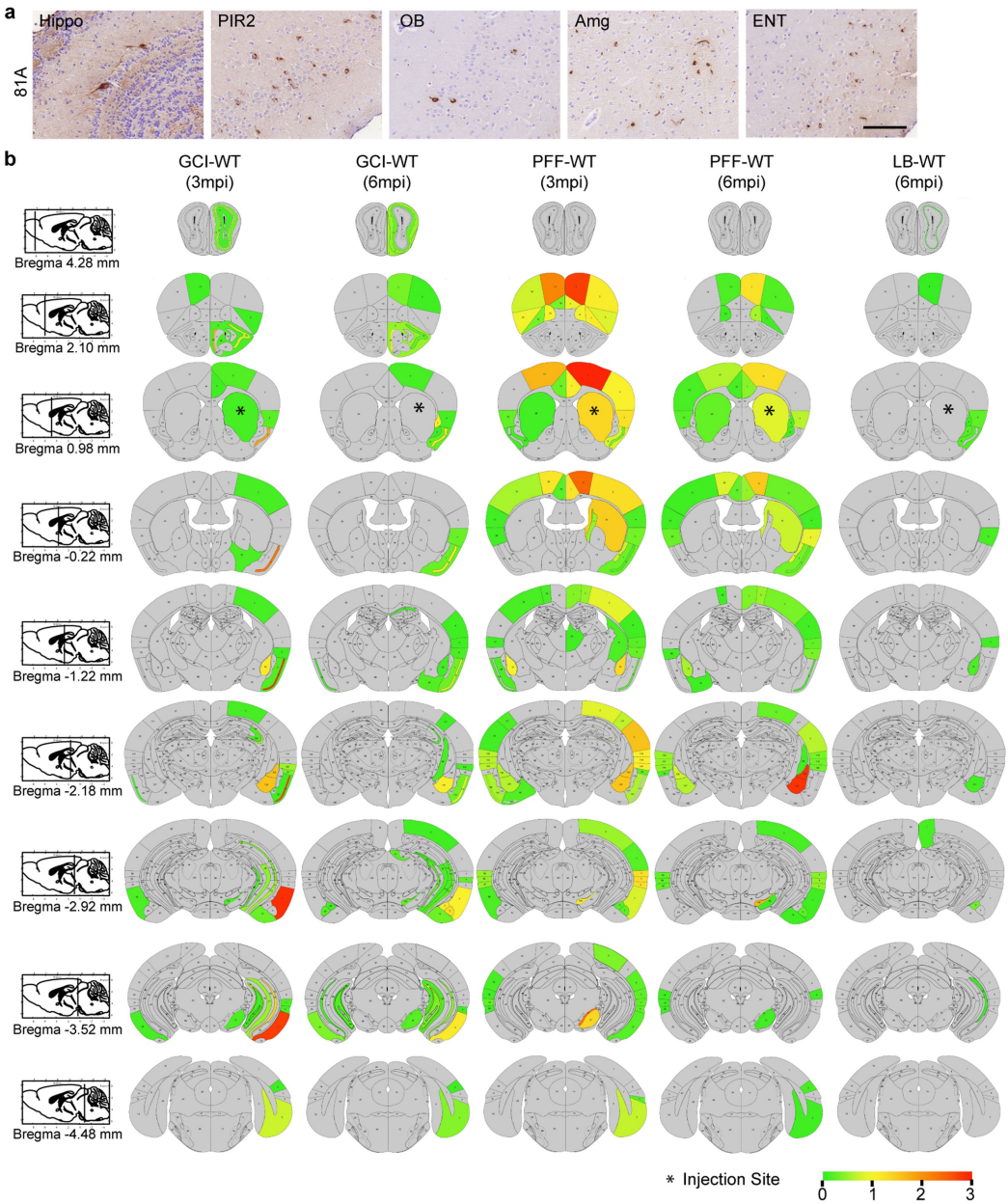

Extended Data Fig. 5 | Distribution of α-Syn pathology in injected wild-type mice. a, Representative photomicrographs of α-Syn pathologies stained by an antibody against pS129 α-Syn (81A) in multiple brain regions in GCI-α-Syn injected wild-type mice (experiment repeated three times). **b**, Heat map for the distribution of α-Syn pathology in wild-type mice injected with GCI-α-Syn, PFF or LB-α-Syn. GCI-α-Syn, LB-α-Syn and α-Syn PFF were unilaterally injected into the dorsal striatum of wild-type mice. The seeded α-Syn pathology was analysed and graded by immunohistochemistry with Syn506. The data were presented as heat maps to semiquantitatively demonstrate the central nervous system (CNS) distribution of α-Syn pathology. Each panel represents a coronal plane (bregma 4.28, 2.10, 0.98, −0.22, −1.22,−2.18, −2.92, −3.52 and −4.48 mm) for each treatment group (GCI-WT, $n = 3$ mice; PFF-WT, $n = 4$ mice; LB-WT, $n = 3$ mice). Scale bar: 100 μm.

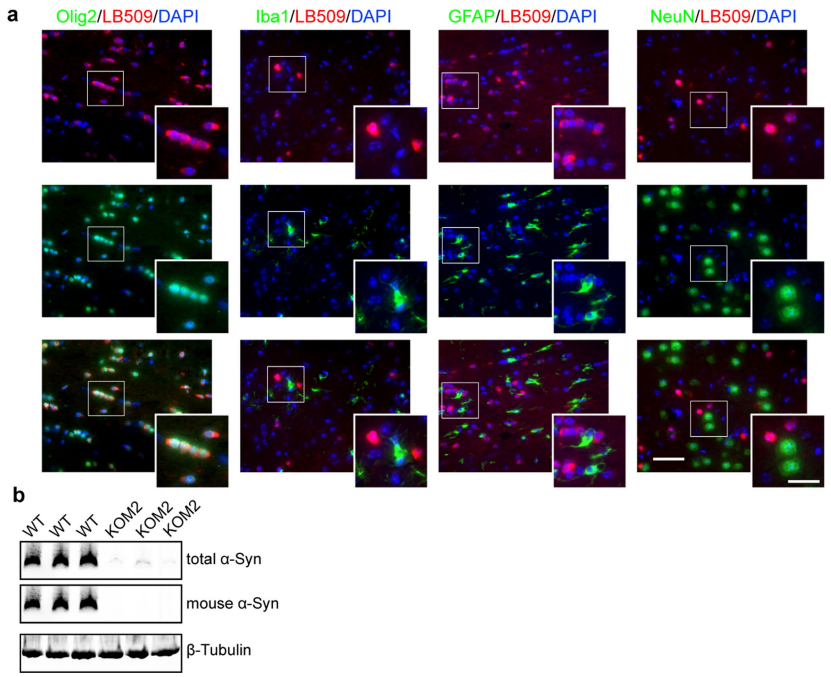

Extended Data Fig. 6 | Characterization of KOM2 mice. a, Brain sections from KOM2 mice were double-labelled with antibodies against α-Syn (LB509) and various cell-type specific markers: Olig2 (oligodendrocytes), Iba1 (microglial cells), GFAP (astrocytes) and NeuN (neurons). In KOM2 mice, α-Syn is expressed only in oligodendrocytes. **b**, Brain lysates of wild-type and KOM2 mice were immunoblotted with an antibody against total α-Syn (Syn 9027), mouse α-Syn (Cell Signalling) and β-tubulin. Scale bars: 50 μm (**a**), 25 μm (**a** inset). The experiments in **a**, **b** have been repeated three times with similar results. For gel source data, see Supplementary Fig. 1.

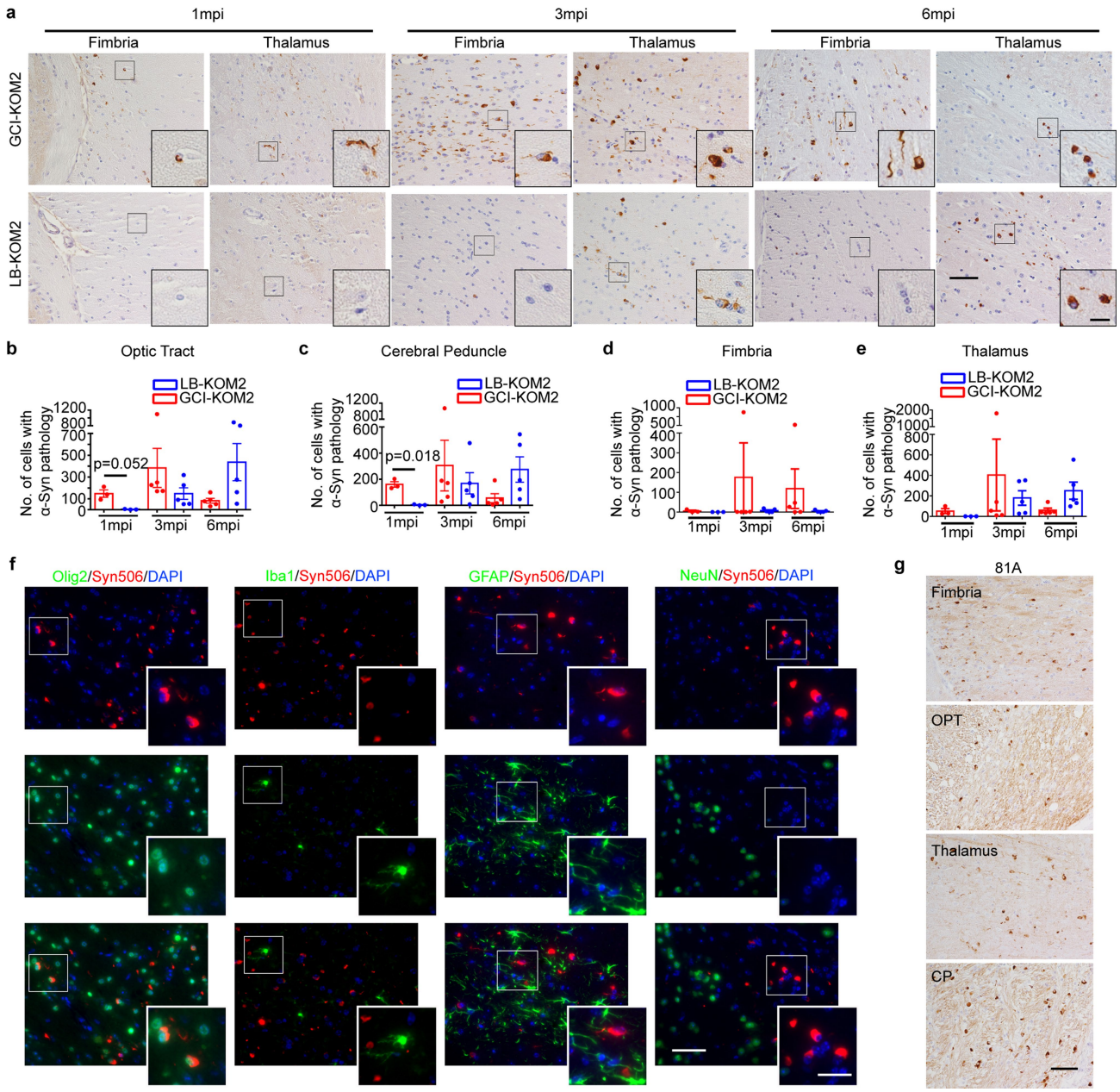

Extended Data Fig. 7 | Induction of oligodendroglial α-Syn pathology in KOM2 mice. a, Syn506-positive α-Syn aggregates seeded by equal amounts of GCI-α-Syn or LB-α-Syn (18.75 ng) in KOM2 mice at one, three and six month post-injection in fimbria and thalamus. **b**–**e**, Quantification of the number of oligodendrocytes with α-Syn pathology in the optic tract (**b**), cerebral peduncle (**c**), fimbria (**d**), and thalamus (**e**) at different time points (one month post-injection, $n = 3$ mice; three and six months post-injection, $n = 5$ mice). **f**, Brain sections from GCI-α-Syn injected KOM2 mice were double-labelled with antibodies against misfolded α-Syn (Syn506) and various cell-type specific markers. The induced α-Syn pathologies are located in oligodendrocytes in KOM2 mice. **g**, GCI-α-Syn-injected KOM2 mouse brain sections were stained with an antibody against phosphorylated α-Syn (81A). Results shown as mean ± s.e.m. Scale bars: 50 μm (**a**, **f** and **g**), 12.5 μm (**a** insets) and 25 μm (**f** insets). The experiments in **a**, **f** and **g** have been repeated three times with similar results. Statistics shown in **b**, **c** are two tailed unpaired *t*-test adjusted with Bonferroni correction. See Supplementary Table 5 for statistical details.Source Data

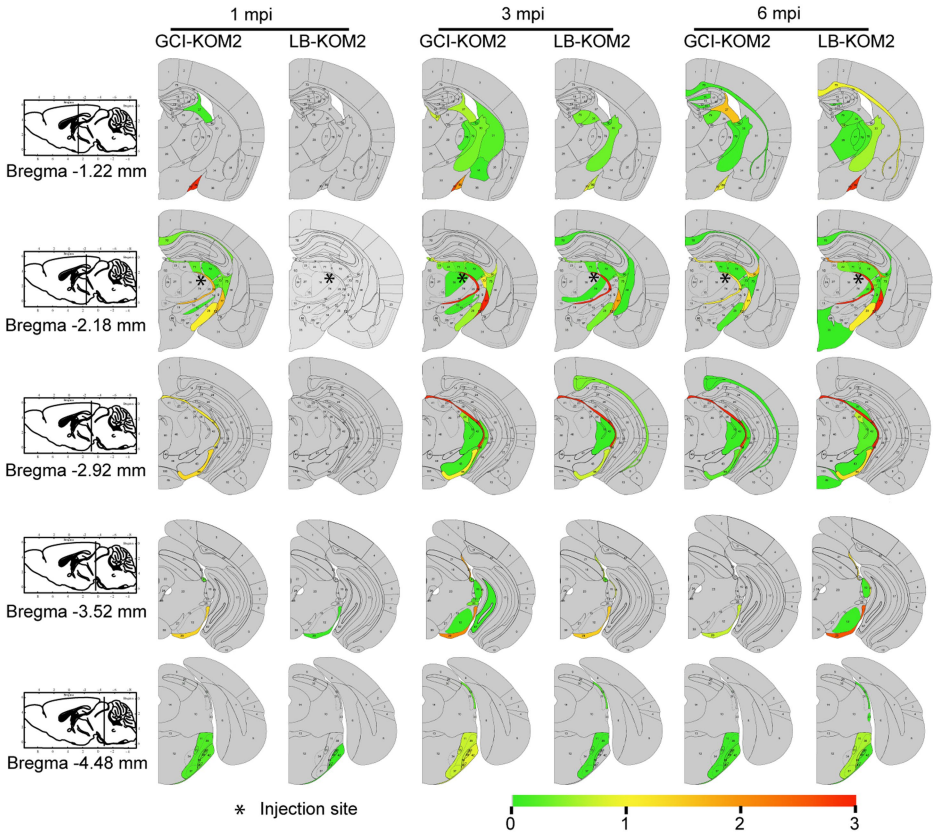

Extended Data Fig. 8 | Distribution of α-Syn pathology in injected KOM2 mice. Heat maps to semiquantitatively demonstrate the CNS distribution of α-Syn pathology in KOM2 mice unilaterally injected with GCI-α-Syn or LB-α-Syn into the thalamus. α-Syn pathologies were analysed and graded by immunohistochemistry with Syn506 at one month ($n = 3$), three months ($n = 5$) and six month ($n = 5$) post injection. Each panel represents a coronal plane (bregma −1.22, −2.18, −2.92, −3.52, −4.48 mm) for each treatment group. Because there is no α-Syn pathology in the contralateral side, only the ipsilateral side is shown.

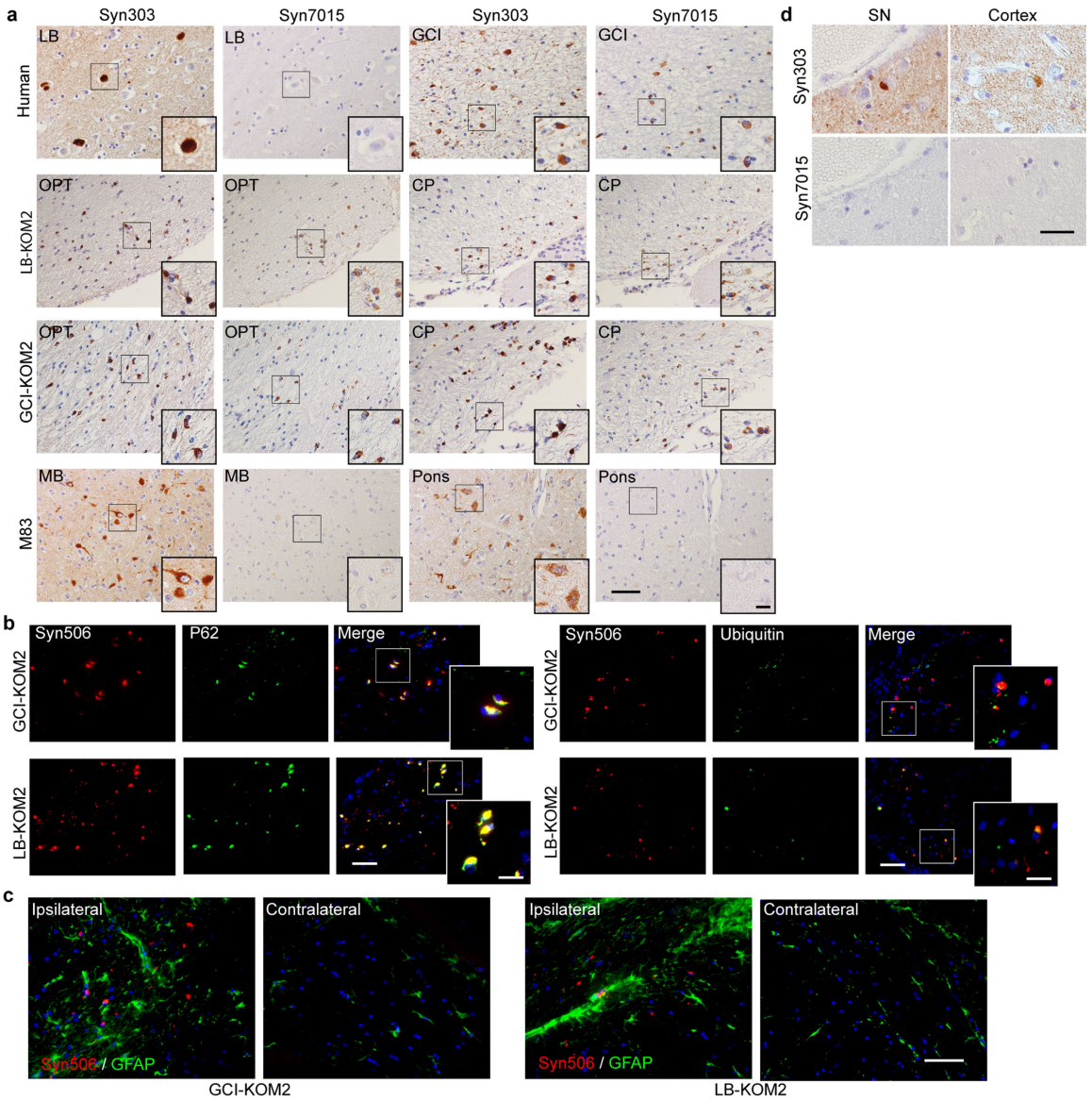

Extended Data Fig. 9 | Oligodendrocyte environment generates the GCI-α-Syn strain. a, Immunohistochemistry of adjacent sections from human or mouse brains with Syn303 and Syn7015. First row, adjacent brain sections of cases of Lewy body disease and MSA used for the extraction of LB-α-Syn and GCI-α-Syn for injection. Second row, adjacent brain sections of KOM2 mice injected with LB-α-Syn prepared from the brain tissue shown in the first row. OPT and CP are shown. Whereas the LB-α-Syn used for the injections is Syn7015-negative, the oligodendrocyte pathology that is induced is Syn7015-positive. Third row, adjacent brain sections of KOM2 mice injected with GCI-α-Syn prepared from the brain sample shown in the first row. OPT and CP are shown. Fourth row, adjacent brain sections of M83 mice with α-Syn pathology. Midbrain (MB) and pons are shown. **b**, Brain sections from KOM2 mice injected with GCI-α-Syn or LB-α-Syn in the thalamus were double-labelled with Syn506 and antibodies against P62 (left panel) or ubiquitin (right panel). **c**, Brain sections from GCI-α-Syn- or LB-α-Syn-injected KOM2 mice were double-labelled with Syn506 and GFAP. Both ipsilateral and contralateral optic tracts are shown. **d**, Adjacent sections of substantia nigra and cortex from two different cases of MSA were stained with Syn7015 and Syn303. Scale bars: 50 μm (**a**–**c**), 12.5 μm (**a** insets), 20 μm (**b** inset) and 30 μm (**d**). The experiments in **a**–**d** have been repeated three times with similar results.

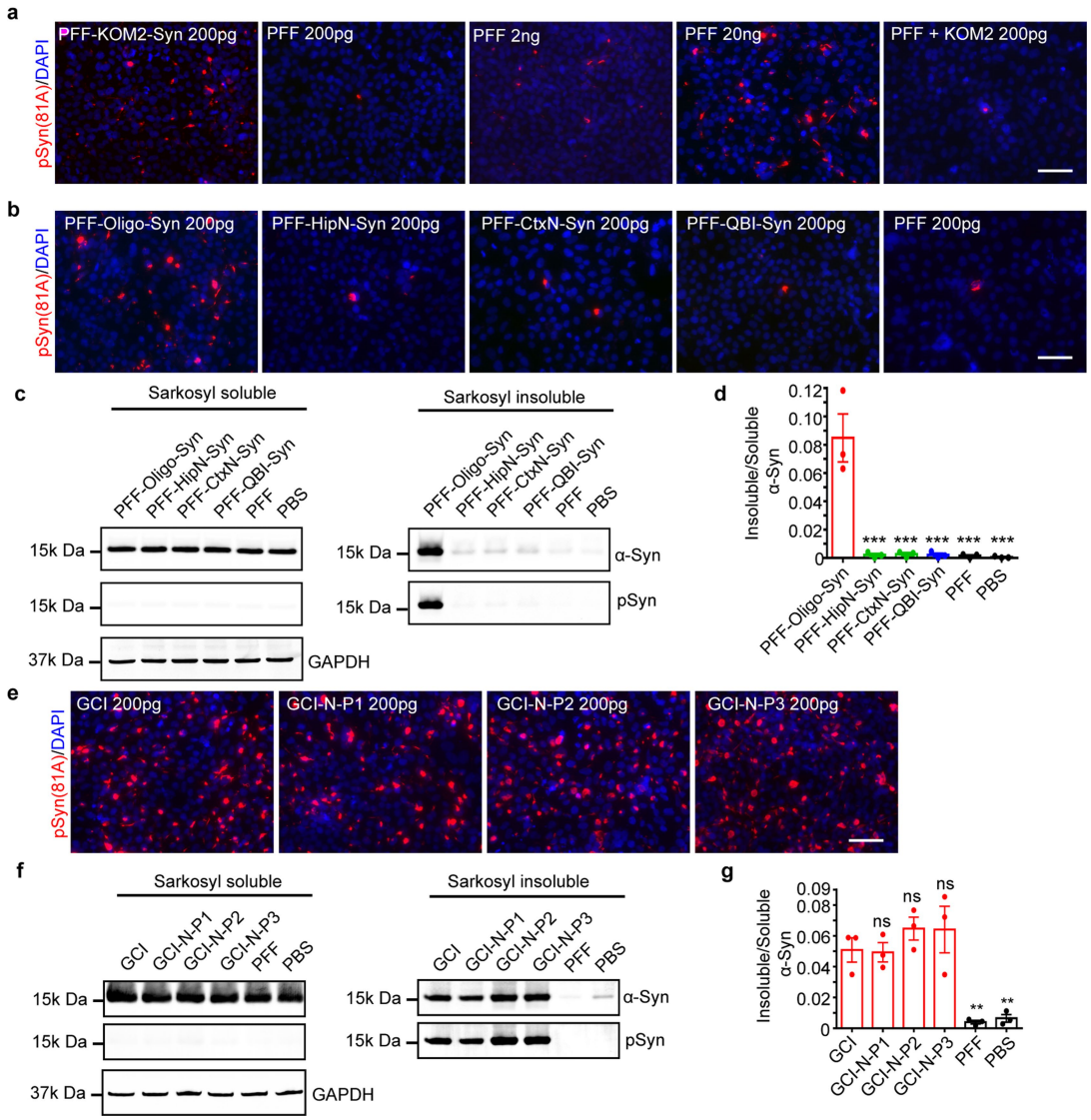

Extended Data Fig. 10 | α-Syn pathology induced by passaged PFF and GCI. a, Insoluble phosphorylated α-Syn in QBI-WT-Syn cells seeded by PFFs, PFFs that have been passaged in KOM2 mice (PFF-KOM2-Syn) or PFFs that were combined with the sarkosyl-insoluble fraction prepared from uninjected KOM2 mice (PFF + KOM2). **b**, Insoluble phosphorylated α-Syn in QBI-WT-Syn cells induced by an equal amount (200 pg) of PFF-oligo-Syn, PFF-HipN-Syn, PFF-CtxN-Syn, PFF-QBI-Syn and PFFs. **c**, Soluble and insoluble fractions from QBI-Syn-WT cells treated with the same amount of PFF-oligo-Syn, PFF-HipN-Syn, PFF-CtxN-Syn, PFF-QBI-Syn and PFF were immunoblotted with antibodies against total or pS129 α-Syn. **d**, Densitometric quantification of insoluble versus soluble α-Syn for experiments described in **c** ($n = 3$ biological replicates). **e**, Insoluble phosphorylated α-Syn in QBI-WT-Syn cells induced by GCI-α-Syn and GCI-α-Syn that has been passaged in primary neurons for multiple times (that is, GCI-N-P1, GCI-N-P2, GCI-N-P3). **f**, Soluble and insoluble fractions from QBI-Syn-WT cells treated with the same amount of GCI, GCI-N-P1, GCI-N-P2, GCI-N-P3 and PFF were immunoblotted with antibodies against total α-Syn or pS129 α-Syn. **g**, Densitometric quantification of insoluble versus soluble α-Syn for experiments described in **f** ($n = 3$ biological replicates). Statistics shown in **d**, **g** are one-way ANOVA followed by Dunnett's post hoc test comparing each group with PFF-oligo-Syn in **d** or GCI in **g**. Results shown as mean ± s.e.m. $^{**}P < 0.01$; $^{***}P < 0.01$; ns, not significant. Scale bars: 50 μm (**a**, **b**, **e**). The experiments in **a**–**c** and **e**–**f** have been repeated three times with similar results. See Supplementary Table 5 for statistical details. For gel source data, see Supplementary Fig. 1.Source Data

nature research

Corresponding author(s): Virginia M.-Y. Lee

☐ Initial submission ☐ Revised version ☒ Final submission

Life Sciences Reporting Summary

Nature Research wishes to improve the reproducibility of the work that we publish. This form is intended for publication with all accepted life science papers and provides structure for consistency and transparency in reporting. Every life science submission will use this form; some list items might not apply to an individual manuscript, but all fields must be completed for clarity.

For further information on the points included in this form, see Reporting Life Sciences Research. For further information on Nature Research policies, including our data availability policy, see Authors & Referees and the Editorial Policy Checklist.

Experimental design

1. Sample size

Describe how sample size was determined.

Sample sizes were selected based on previous experience to obtain statistical significance and reproducibility.

2. Data exclusions

Describe any data exclusions.

No data has been excluded

3. Replication

Describe whether the experimental findings were reliably reproduced.

All the experimental findings were reliably reproduced

4. Randomization

Describe how samples/organisms/participants were allocated into experimental groups.

For all animal studies, mice were randomly assigned to each group.

5. Blinding

Describe whether the investigators were blinded to group allocation during data collection and/or analysis.

The investigators were blinded to group allocation for quantitative analysis.

Note: all studies involving animals and/or human research participants must disclose whether blinding and randomization were used.

6. Statistical parameters

For all figures and tables that use statistical methods, confirm that the following items are present in relevant figure legends (or in the Methods section if additional space is needed).

n/a	Confirmed
☐	☒ The exact sample size (*n*) for each experimental group/condition, given as a discrete number and unit of measurement (animals, litters, cultures, etc.)
☐	☒ A description of how samples were collected, noting whether measurements were taken from distinct samples or whether the same sample was measured repeatedly
☐	☒ A statement indicating how many times each experiment was replicated
☐	☒ The statistical test(s) used and whether they are one- or two-sided (note: only common tests should be described solely by name; more complex techniques should be described in the Methods section)
☐	☒ A description of any assumptions or corrections, such as an adjustment for multiple comparisons
☐	☒ The test results (e.g. *P* values) given as exact values whenever possible and with confidence intervals noted
☐	☒ A clear description of statistics including central tendency (e.g. median, mean) and variation (e.g. standard deviation, interquartile range)
☐	☒ Clearly defined error bars

See the web collection on statistics for biologists for further resources and guidance.

Software

Policy information about availability of computer code

7. Software

Describe the software used to analyze the data in this study.	Graphpad Prism version 7.03, HALO version 2.0.106.3, In Cell Developer Toolbox version 1.7 and Image Studio version 2.0.38 were used to analyze the data.

For manuscripts utilizing custom algorithms or software that are central to the paper but not yet described in the published literature, software must be made available to editors and reviewers upon request. We strongly encourage code deposition in a community repository (e.g. GitHub). *Nature Methods* guidance for providing algorithms and software for publication provides further information on this topic.

Materials and reagents

Policy information about availability of materials

8. Materials availability

Indicate whether there are restrictions on availability of unique materials or if these materials are only available for distribution by a for-profit company.	no restrictions

9. Antibodies

Describe the antibodies used and how they were validated for use in the system under study (i.e. assay and species).

81A, anti-Ser129 phosphorylated alpha-Synuclein antibody, was in house generated and validated before (Waxman and Giasson, 2008). It was used at 1:5000 for immunocytochemistry (ICC), 1:1000 for western blot (WB) and 1:10000 for immunohistochemistry (IHC).
SNL-4, anti-alpha-Synuclein (amino acids 2-11) antibody, was in house generated and validated before (Giasson et al., 1999). It was used at 1:500 for WB.
Syn506, anti-misfolded alpha-Synuclein antibody, was in house generated and validated before (Waxman and Giasson, 2008). It was used at 1:5000 for IHC and 1:2500 for immunofluorescent (IF) staining.
NAC1, anti-alpha-Synuclein (amino acids 75-91) antibody, was in house generated and validated before(Giasson et al., 2001). It was used at 1:500 for WB.
LB509, anti-alpha-Synuclein (amino acids 115-122) antibody, was in house generated and validated before (Jakes et al., 1999). It was used at 1:500 for WB and 1:2500 for IF.
Syn211, anti-alpha-Synuclein (amino acids 121-125) antibody, was in house generated and validated before(Giasson et al., 2000). It was used at 1:500 for WB.
Syn102, anti-alpha-Synuclein (amino acids 131-140) antibody, was in house generated and validated before (Tu et al., 1998). It was used at 1:500 for WB.
HuA, anti-alpha-Synuclein antibody, was in house generated and validated before (Murray et al., 2003). It was used at 3.3ng/ l for ELISA and 1:500 for WB.
Syn9027, anti-alpha-Synuclein antibody (amino acids 130-140), was in house generated and validated before(Covell et al., 2017). It was used at 3.3ng/ l for ELISA and 1:20000 for WB.
MJF-R1, anti-human alpha-Synuclein antibody was from Abcam (ab138501) and validated by Abcam. It was used at 1:1000 for ELISA.
SNL-1, anti-alpha-Synuclein (C-terminal) antibody, was in house generated and validated before (Giasson et al., 1999). It was used at 1:500 for WB.
Olig-2, anti-Oligodendrocyte transcription factor 2 antibody, was from Millipore (AB9610) and validated by Millipore. It was used at 1:500 for IF and ICC.
Iba1, anti-Macrophage/Microglia-Specific Calcium-Binding Protein antibody, was from Wako (019-19741) and validated by Wako. It was used at 1:500 for IF and ICC.
GFAP, anti-Glial Fibrillary Acidic Protein anibody, was from Dako (Z0334) and validated by Dako. It was used at 1:1000 for IF and 1:500 for ICC.
NeuN, anti-Neuronal Nuclei antibody, was from Millipore (ABN78) and validated by Millipore. It was used at 1:1000 for IF and 1:500 for ICC.
MAP2, anti- Microtubule-Associated Protein 2 antibody, was in house generated and validated before (Giasson et al., 1999). It was used at 1:2000 for ICC.
PLP, anti-proteolipid protein antibody, was a kind gift from Dr. Judith B. Grinspan. The antibody was originally from Dr. Alex Gow, Wayne State University, Detroit, MI and has been validated before (Reid et al., 2012). It was used at 1:1 for ICC.
CNP. Anti-2',3'-Cyclic-nucleotide 3'-phosphodiesterase antibody, was in house generated and validated before (Yazawa et al., 2005). It was used at 1:500 for ICC.
Syn204, anti-alpha-Synuclein (amino acids 87-110) antibody, was in house generated and validated before (Giasson et al., 2000). It was used at 1:500 for WB.
Syn303, anti-alpha-Synuclein (amino acids 87-110) antibody, was in house generated and validated before (Duda et al., 2002). It was used at 1:60000 for IHC.
Syn7015, anti-alpha-Synuclein antibody, was in house generated and validated before(Covell et al., 2017). It was used at 1ng/ml for IHC.
Mouse α-syn, anti-mouse α-syn antibody, was from Cell Signaling Technology (4179) and validated by Cell Signaling Technology. It was used at 1:1000 for WB.
β-tubulin, anti-β-tubulin antibody, was from Invitrogen (32-2600) and validated by Invitrogen. It was used at 1:3000 for WB.
GAPDH, anti-GAPDH antibody, was from Advanced Immunochemical (2-RGM2) and validated by Advanced Immunochemical. It was used at 1:18000 for WB.

10. Eukaryotic cell lines

a. State the source of each eukaryotic cell line used.

QBI-WT-Syn Cell line is generated from QBI cells to stably express human wild type α-Synuclein. Primary neurons culture were generated from wild-type mouse or rat embryos. Primary oligodendrocyte culture were generated from wild-type new born rats.

b. Describe the method of cell line authentication used.

Cell line authentication was not performed as cells were not listed in the commonly misidentified category.

c. Report whether the cell lines were tested for mycoplasma contamination.

All cells were mycoplasma-free.

d. If any of the cell lines used are listed in the database of commonly misidentified cell lines maintained by ICLAC, provide a scientific rationale for their use.

These cells are not in the database

Animals and human research participants

Policy information about studies involving animals; when reporting animal research, follow the ARRIVE guidelines

11. Description of research animals

Provide details on animals and/or animal-derived materials used in the study.

2-3 months old C57BL6/C3H wild-type mice were purchased from Charles River. M2 mice expressing wild type human α-Synuclein in oligodendrocytes under the control of CNP promoter have been described previously. KOM2 mice were generated by crossing M2 mice with Snca-/- mice. 3-4 months old KOM2 has been used for the study. All breeding, housing, and experimental procedures were performed according to the NIH Guide for the Care and Use of Experimental Animals and approved by the University of Pennsylvania Institutional Animal Care and Use Committee (IACUC). Both male and female mice were used for this study.

Policy information about studies involving human research participants

12. Description of human research participants

Describe the covariate-relevant population characteristics of the human research participants.

No living patients participated in this study. The human postmortem samples used here were from the brain bank at Center for Neurodegenerative Disease Research at the University of Pennsylvania. Details can be found here: http://www.med.upenn.edu/cndr/biosamples-brainbank.html. Demographics of human postmortem cases used in this study are detailed in Supplementary Table 1 and 2.